

Performance and Reliability Analysis for Practical Byzantine Fault Tolerance with Repairable Voting Nodes

Yan-Xia Chang¹, Qing Wang², Quan-Lin Li^{1*}, Yaqian Ma¹

¹School of Economics and Management

Beijing University of Technology, Beijing 100124, China

²Monash Business School

Monash University, Melbourne, Australia

June 21, 2023

Abstract

The practical Byzantine fault tolerant (PBFT) consensus protocol is one of the basic consensus protocols in the development of blockchain technology. At the same time, the PBFT consensus protocol forms a basis for some other important BFT consensus protocols, such as Tendermint, Streamlet, HotStuff, and LibraBFT. In general, the voting nodes may always fail so that they can leave the PBFT-based blockchain system in a random time interval, making the number of timely available voting nodes uncertain. Thus, this uncertainty leads to the analysis of the PBFT-based blockchain systems with repairable voting nodes being more challenging. In this paper, we develop a novel PBFT consensus protocol with repairable voting nodes and study such a new blockchain system using a multi-dimensional Markov process and the first passage time method. Based on this, we provide performance and reliability analysis, including throughput, availability, and reliability, for the new PBFT-based blockchain system with repairable voting nodes. Furthermore, we provide an approximate algorithm for computing the throughput of the new PBFT-based blockchain system. We employ numerical examples to demonstrate the validity of our theoretical results

*Corresponding author: Q. L. Li (liquanlin@bjut.edu.cn)

This work has been submitted to the IEEE for possible publication. Copyright may be transferred without notice, after which this version may no longer be accessible.

and illustrate how the key system parameters influence performance measures of the PBFT-based blockchain system with repairable voting nodes. We hope the methodology and results developed in this paper will stimulate future research endeavors and open up new research trajectories in this field.

Keywords: Practical Byzantine fault tolerance (PBFT); Blockchain; Repairable voting nodes; Queueing system; Performance evaluation; Reliability.

1 Introduction

As one of the fundamental problems in computer science, the consensus problem in distributed computing field was first raised by Pease, Shostak, and Lamport [1] in 1980, and the later was named “The Byzantine General problem” by [2, 3]. Along with computer development, the consensus problem has received more attention over the last decade due to its extensive applications to a new distributed system called “blockchain” such as Bitcoin [4] and Ethereum [5]. Driven by the opportunities in the concept of cryptocurrencies and blockchain, a variety of consensus has emerged [6, 7], where BFTs or PBFTs play a crucial role in the evolution of the blockchain ledger consensus.

In contrast to public blockchains such as Bitcoin [4] and Ethereum 1.0 [5], which are based on Proof-of-Work (PoW) consensus protocol, PBFT-based blockchain system tends to have only a subset of participating nodes running the PBFT protocol. Those nodes can be tightly controlled by the membership, and once more than $2/3$ of the voting nodes have approved a proposal proposed by the primary node, a round of voting consensus is reached. For such a PBFT-based blockchain system that allows less than $1/3$ of voting nodes to fail due to some reasons, it can work correctly even under malicious attacks, software errors, operator mistakes, and so on. Based on this fault-tolerant capability, the PBFT-based blockchain has some advantages, such as access control, low energy consumption, high throughput, fast consensus speed, and high scalability. For more details, readers may refer to several survey papers by, for example, Correia et al. [8], Vukolić [9], Gramoli [10], Berger and Reiser [11], Gupta et al. [12], Stifter et al. [13], Alqahtani and Demirbas [14], Zheng and Feng [15], Gan et al. [16] and others.

Although PBFT-based blockchain systems offer the above advantages, it also has some limitations. For example, an ordinary PBFT-based blockchain has poor system flexibility. In other words, the voting nodes cannot freely join or exit the PBFT network. Therefore,

it is impossible for a more general PBFT-based blockchain system to take into account the behavior of failed nodes who leave the PBFT-based blockchain system or of repaired nodes who reconnect to the PBFT network. This limitation goes against the principle that all the nodes of the PBFT-based voting network have the right to vote on a proposal or suggestion over time. Also, if more than $1/3$ of nodes fail, and the failed nodes have not been repaired in a timely manner, then the PBFT-based blockchain system will never reach a consensus. Obviously, this limitation is also harmful to the liveness, availability, and security of the PBFT-based blockchain system. Thus, it is necessary to consider a new PBFT consensus protocol, in which the failed nodes may leave the PBFT network, while the repaired nodes can re-enter the PBFT network. By introducing a failure and repair process, the nodes that fail and repair can change the number of voting nodes in the PBFT network, allowing us to observe the availability and security of the PBFT-based blockchain system in a timely manner. In addition, the inclusion of repaired nodes allows the PBFT network to perform the voting consensus, even if the PBFT-based blockchain system is on the verge of becoming unavailable due to the larger number of failed nodes in the system.

In this paper, we focus on the PBFT-based blockchain system with repairable voting nodes and provide performance and reliability analysis for such a new blockchain system using a multi-dimensional Markov process and the first passage time method. Meanwhile, we develop some key performance and reliability measures for the PBFT-based blockchain system with repairable voting nodes, including throughput, availability, and reliability. These are all important measures to describe and evaluate blockchain systems. Note that in our paper, the Markov processes and queueing theory play a key role in the study of PBFT-based blockchain systems. A growing body of literature has applied Markov processes and queueing theory to study blockchain systems. For example, a simple Markov chain by Eyal and Sirer [17], a Markov queueing model by Li et al. [18, 19], a two-dimensional Markov process by Göbel et al. [20] and Javier and Fralix [21], a pyramid Markov process by Li et al. [22], a Markov process of DAG-based blockchain by Song et al. [23], a Markov process of PBFT-based blockchain by Ma et al. [24], and a Markov queueing model of dynamic PBFT-based blockchain system by Chang et al. [25] and so on. From those works, it becomes evident that Markov processes and queueing theory can well describe some different consensus processes of blockchain systems, and they can have universality and superiority in evaluating the performance measures of blockchain

systems.

This paper is closely related to Ma et al. [24], Chang et al. [25], Nischwitz et al. [26], and Hao et al. [27], which provided performance analysis for the PBFT-based blockchain systems by using Markov processes or probabilistic models. Hao et al. [27] presented a dynamic PBFT-based blockchain system with an uncertain number of voting nodes, in which some nodes may enter or leave the PBFT network by means of the JOIN and EXIT protocols. Similarly, Chang et al. [25] described and analyzed the dynamic (entering and leaving) behavior of some nodes in the PBFT network by using the Markov process theory and an approximate queueing system. Compared with Hao et al. [27] and Chang et al. [25], this paper uses a three-dimensional Markov process to describe and analyze the behavior of failed nodes who leave the PBFT network and of repaired nodes who re-enter the PBFT network while the total number of voting nodes (including the failed nodes) is fixed. Based on this, we obtain the probability distributions of block-generated and orphan-block-generated are of phase-type, and then we analyze the throughput of the PBFT-based blockchain system. Differently with this paper, Chang et al. [25] provided a steady-state rate approximate method such that the block generation time and the orphan block generation time were exponential, and then they set up an approximate queueing model to compute the throughput of the PBFT-based blockchain system. Ma et al. [24] adopted a two-dimensional Markov process to describe the voting process, which can be considered a simple and special case of our works. Nischwitz et al. [26] used a probabilistic model to evaluate BFT protocols in the presence of dynamic link and crash failures, which is different from the methodology of this paper.

Based on the above analysis, the main contributions of this paper are summarized as follows:

1. We propose a new PBFT consensus protocol to generalize the ordinary PBFT consensus protocol, in which the failed nodes may leave the PBFT network and some repaired nodes can enter the PBFT network again, so the number of available voting nodes is variable over time. Based on this, we propose a large-scale Markov modeling technique to analyze the performance and reliability of the new PBFT-based blockchain system with repairable voting nodes.
2. We use PH distributions of finite size to express the probability distributions of block-generated and orphan-block-generated times. Then we use the two PH distributions

to set up a more realistic queueing model $M \oplus PH^b / PH^b / 1$ to compute the throughput of the PBFT-based blockchain system with repairable voting nodes, and provide an approximate algorithm for computing the throughput of the PBFT-based blockchain system.

3. We provide reliability analysis for the PBFT-based blockchain systems with repairable voting nodes and expressions for availability, reliability, and the average time before the first failure.
4. We use numerical examples to validate our theoretical results and demonstrate the impact of key parameters on performance measures of the PBFT-based blockchain system with repairable voting nodes.

The structure of this paper is organized as follows. Section 2 surveys related literature on the performance evaluation of PBFT-based blockchain systems. Section 3 describes a new PBFT-based blockchain system with repairable voting nodes. Section 4 analyzes the probability distributions of block-generated and orphan-block-generated times by means of two phase-type distributions of finite sizes. Section 5 introduces queueing model $M \oplus PH^b / PH^b / 1$ to provide performance analysis for the PBFT-based blockchain system with repairable voting nodes. Section 6 sets up two new Markov processes to analyze the reliability of the PBFT-based blockchain systems with repairable voting nodes. Section 7 uses some numerical examples to indicate how the key parameters influence the performance measures of the PBFT-based blockchain system with repairable voting nodes. Section 8 gives some concluding remarks. Finally, two appendixes provide the non-zero matrix elements or blocks in two important infinitesimal generators.

2 Literature Review

In this section, we divide current research into three literature streams: The first is the research on the development and optimization of the PBFT consensus protocol. The second is on analytical models to evaluate the performance of PBFT-based blockchain systems. The third is on simulation models to study the performance of PBFT-based blockchain systems.

(a) Research on the development and optimization of the PBFT consensus protocol

Since Lamport, Shostak, and Pease [1] proposed the Byzantine General problem in 1982, there has been a growing demand to deploy BFT and/or its variations into practical applications. This demand has driven the continuous design and improvement of BFT protocol as well as extensive research utilizing the BFT algorithm. Important examples include Schlichting and Schneider [28], Reischuk [29], Martin and Alvisi [30], Veronese et al. [31], Malkhi et al. [32] and so on. However, many assumptions of some early studies were too idealistic to be realized in reality. To make the BFT protocol more suitable for practical applications, Castro and Liskov [33, 34] improved the BFT and proposed the PBFT protocol, which is the first practical solution to the Byzantine problem and can work in asynchronous environments. Henceforward, some researchers have further developed the BFT or PBFT, effectively improving the performance of the BFT-based protocol. These solutions include but are not limited to dividing replicas into groups [35, 36], introducing hierarchical structure [36], simplifying the PBFT process [37, 38, 39, 40], introducing credit mechanism [35, 38, 41, 42, 43, 44], using multiple consensus in different cases [35, 45, 46], and introducing geography factors [47, 48].

Inspired by these solutions, this paper proposes a new PBFT consensus protocol with repairable voting nodes, which is different from the static PBFT protocol described in the literature above. In such a blockchain system based on this new protocol, failed nodes may leave the PBFT network, and some repaired nodes can enter the PBFT network again. By introducing the fail and repair processes, failed and repaired nodes can change the number of voting nodes in the PBFT network, thus transforming the PBFT protocol from a completely closed environment to an open one. While we hope that the new proposed PBFT can inherit the advantages of the previous PBFT, we also hope that this PBFT-based blockchain system with repairable voting nodes can guarantee liveness, availability, and security.

(b) Research on the performance evaluation based on analytical models

As one of the core components of a blockchain system, the PBFT consensus protocol directly affects the overall throughput, delay, reliability, and fault tolerance of the blockchain system, and determines the efficiency and scalability of a blockchain system to a large extent. Up to now, BFT or PBFT protocol has become the most basic one in all the blockchain consensus mechanisms and has been used in many areas, such as the Internet of Things (IoT) [48, 49, 50], Internet of vehicles (IoV) [51], cloud computing [52], energy trading [53], and many other fields. As more PBFT-based protocols are applied

to reality, evaluating the performance of these blockchain systems becomes increasingly important, which is the first important thing we did after proposing the new PBFT consensus protocol with repairable voting nodes. Readers may refer to the surveys of Fan et al. [54] and Dabbagh et al. [55] for the methods used in recent years to evaluate the performance of PBFT-based blockchain systems.

As we all know, the analytical model mainly starts from the blockchain system itself, which helps to deeply understand the influencing factors, evolution, and development of the blockchain system. Based on this characteristic, these analytical methods can evaluate, interpret, and predict the behavior of PBFT-based blockchain systems. Among studies using analytical models, the closest works to ours are Chang et al. [25], Ma et al. [24], Nischwitz et al. [26], and Hao et al. [27], in which Markov processes or probabilistic models were introduced to evaluate the performance of the PBFT-based blockchain systems. Chang et al. [25] set up a large-scale Markov process to describe a novel dynamic PBFT where the voting nodes may always leave the network while new nodes may also enter the network and provided an effective computational method for the throughput. Ma et al. [24] described a simple stochastic performance model to analyze the voting process of the PBFT-based blockchain system. Nischwitz et al. [26] used a probabilistic model to evaluate BFT protocols in the presence of dynamic links and crash failures. Hao et al. [27] proposed a dynamic PBFT system from the perspective of protocols and used a probabilistic model to calculate the probability that the client gets the correct message. Different from these articles, we not only use the Markov process to analyze the throughput but, in particular, we also analyze the reliability of the PBFT-based blockchain system with repairable voting nodes.

In addition, many researchers have made unremitting efforts to evaluate the performance of PBFT-based blockchain systems from different angles and using various analysis methods. For example, Hao et al. [56] proposed a method to evaluate the performance of PBFT consensus in Hyperledger and showed that PBFT consistently outperforms PoW in terms of latency and throughput under varying workloads. Sukhwani et al. [57] modeled the PBFT consensus process using Stochastic Reward Nets (SRN) to compute the mean time to complete consensus for networks of up to 100 peers. Lorünser [58] presented a performance model for PBFT that specifically considered the impact of unreliable channels and the use of different transport protocols over them. Pongnumkul et al. [59] developed a method to evaluate the Hyperledger Fabric and Ethereum and showed that Hyperledger

Fabric consistently outperforms Ethereum across all evaluation metrics (execution time, latency, and throughput).

(c) Research on the performance evaluation based on simulation models

As one of the commonly used methods to evaluate the performance of blockchain, simulation models are primarily used to simulate or approximate the behavior and development of practical blockchain systems with computers in situations where the description of analytical models is not possible or where it is challenging to set up an analytical model. Based on the simulation models, Meshcheryakov et al. [49] argued the effectiveness of the PBFT consensus algorithm for its implementation on constrained IoT devices, simulated the main distributed ledger scenarios using PBFT, and evaluated the blockchain system performance. Monrat et al. [60] provided a performance and scalability analysis of popular private blockchain platforms by varying the workloads and determining the performance evaluation metrics such as throughput and network latency. Ahmad et al. [61] developed a blockchain test platform to execute and test the latency and throughput of blockchain systems, including PBFT, PoW, Proof of Equity (PoS), Proof of Elapsed Time (PoET), and Clique. Zheng et al. [62] used continuous-time Markov chain (CTMC) models to simulate the time response of a PBFT-based healthcare blockchain network.

From the above literature streams, existing relevant literature has studied the performance of PBFT-based blockchain systems from three aspects: protocol, analytical models, and simulation models. The former focuses on improving the PBFT protocol to evaluate and improve the performance of the PBFT-based blockchain systems from the protocol itself, while the latter two mainly evaluate the performance of the PBFT-based blockchain system from the operating mechanism of the blockchain itself. However, few studies have used the Markov process theory to analyze the performance and reliability of PBFT-based blockchain systems with repairable voting nodes. Motivated by the scarcity of research on the performance and reliability of PBFT-based blockchain systems with repairable voting nodes, we are compelled to develop this topic in this paper.

3 Model Description

In this section, we provide a detailed model description for a PBFT-based blockchain system with repairable voting nodes. Also, we give mathematical notation, random factors, and necessary parameters used in our later study.

(1) The failure process of voting nodes: We assume that each voting node can fail in the PBFT-based blockchain system, and the lifetime of the voting node is exponential with mean $1/\theta > 0$. Once a voting node fails, it cannot handle any other work or task until it is repaired well to enter the working state again.

(2) The repair process of voting nodes: Once any voting node fails, it immediately enters a repair state. We assume that the repair time of the failed voting node is exponential with mean $1/\mu > 0$.

(3) The total number of voting nodes: For the convenience of analysis, we assume that the total number of voting nodes in the PBFT network is a fixed value $N = 3n + 1$, where n is a given positive integer.

(4) The voting process: We assume that the voting time of each node is exponential with mean $1/\gamma > 0$. Additionally, we assume that each node can have only one voting chance with a voting period.

(5) The probability that a transaction package is either approved or disapproved: Using the law of large numbers from some voting statistics, we assume that the probability that each voting node approves a transaction package is p ; while the probability that each voting node disapproves a transaction package is $q = 1 - p$.

(6) The judgment of voting result: We denote by $N(t)$, $M(t)$, and $K(t)$ the number of voting nodes that approve the transaction package, the number of voting nodes that disapprove the transaction package, and the number of failed nodes at time $t > 0$, respectively. Based on this assumption, we judge the voting results in a round of voting process as follows:

(a) If $N(t) = 2n + 1$, then the number of approval votes is more than $2/3$ of the total number of voting nodes. This means that a transaction package can be determined as a block so that the block can be pegged on the blockchain.

(b) If $M(t) + K(t) = n + 1$, then the number of approval votes is less than $2/3$ of the total number of voting nodes. This means that a transaction package can be determined as an orphan block so that the orphan block must be rolled back to the transaction pool to be dealt with again.

(7) The times of pegging a block and rolling back an orphan block: Note that the processes of pegging a block and rolling back an orphan block are all performed in the PBFT-based blockchain network. Thus, we regard the block-pegging time and the orphan block rolling-back time as identical, and we assume that the block-pegging time

and the orphan block rolling-back time are exponential with the mean $1/\beta$.

(8) Independence: We assume that all random variables defined above are independent of each other.

Remark 1 *From Assumption (6), there exist three different cases in which a transaction package is determined as an orphan block: (1) $M(t) = n + 1$, $K(t) = 0$; (2) $M(t) = 0$, $K(t) = n + 1$; (3) $M(t) + K(t) = n + 1$ for $M(t) \geq 1$ and $K(t) \geq 1$.*

Remark 2 *In the process of PBFT voting, once a transaction package is determined as a block (i.e., $N(t) = 2n + 1$), it is not necessary to further perform any subsequent process such that $N(t) > 2n + 1$. Similarly, once a transaction package is determined as an orphan block (i.e., $M(t) + K(t) = n + 1$), it is not necessary to further perform any subsequent process such that $M(t) + K(t) > n + 1$.*

4 Block- and Orphan-Block-Generated Time Distributions

In this section, we express the probability distributions of block- and orphan-block-generated times by means of the phase-type distributions of finite sizes.

Note that $N(t)$, $M(t)$, and $K(t)$ denote the number of voting nodes that approve the transaction package, the number of voting nodes that disapprove the transaction package, and the number of failed nodes at time $t \geq 0$, respectively. It is easy to see that $\{(N(t), M(t), K(t)) : t \geq 0\}$ is a three-dimensional continuous-time Markov process whose state space is given by

$$\Omega = \bigcup_{k=0}^{2n+1} \text{Level } k,$$

where for $0 \leq k \leq 2n$,

$$\begin{aligned} \text{Level } k = & \{(k, 0, 0), (k, 0, 1), \dots, (k, 0, n - 1), (k, 0, n), (k, 0, n + 1) ; \\ & (k, 1, 0), (k, 1, 1), \dots, (k, 1, n - 1), (k, 1, n); \\ & (k, 2, 0), (k, 2, 1), \dots, (k, 2, n - 1); \dots ; \\ & (k, n + 1, 0)\}, \end{aligned}$$

and for $k = 2n + 1$,

$$\begin{aligned} \text{Level } k &= \{(k, 0, 0), (k, 0, 1), \dots, (k, 0, n-2), (k, 0, n-1), (k, 0, n)\}; \\ &\{(k, 1, 0), (k, 1, 1), \dots, (k, 1, n-2), (k, 1, n-1)\}; \\ &\{(k, 2, 0), (k, 2, 1), \dots, (k, 2, n-2)\}; \dots; \\ &\{(k, n, 0)\}. \end{aligned}$$

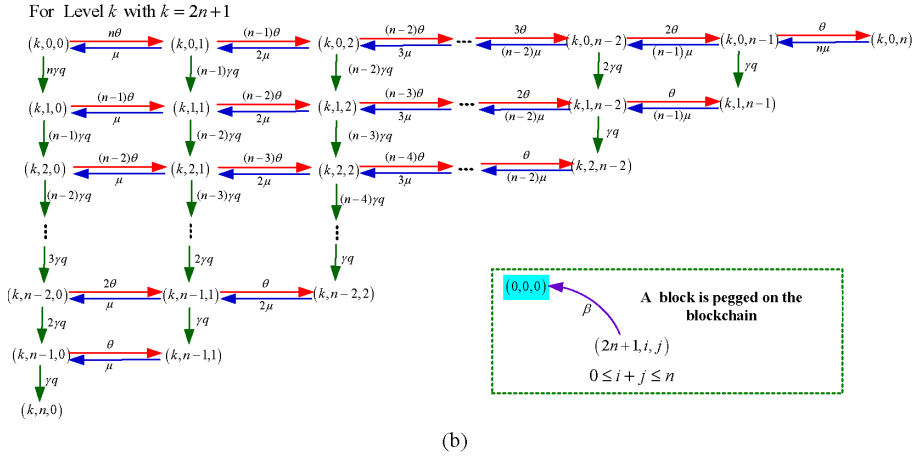
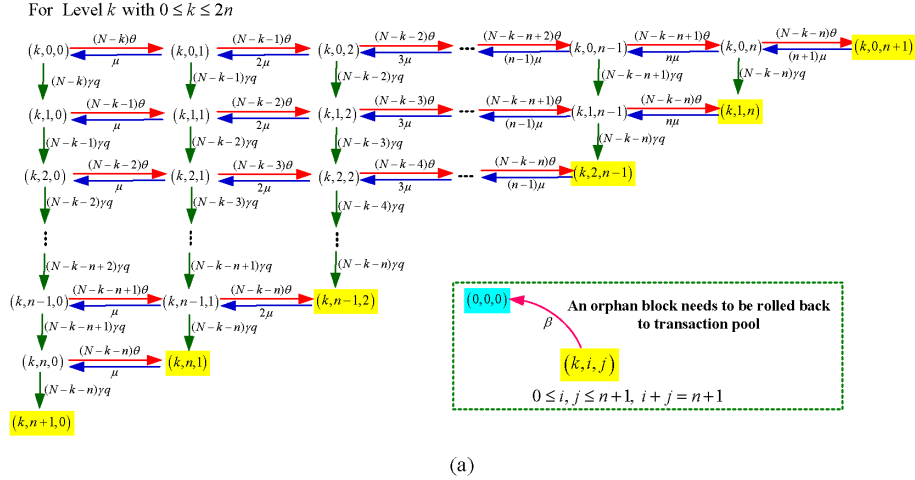


Figure 1: The state transition relations of the Markov process within one level.

In Fig. 1(a), a yellow state (k, i, j) with $i + j = n + 1$ denotes that the transaction package is determined as an orphan block, and it needs to be rolled back to the transaction pool. In Fig. 1(b), each state in Level $(2n + 1)$ is determined as a block, and it can be pegged on the blockchain. Once a transaction package is determined as either a block or

an orphan block, this round of voting process is over. Then, the blockchain system enters the state $(0, 0, 0)$ such that a new round of voting process begins again.

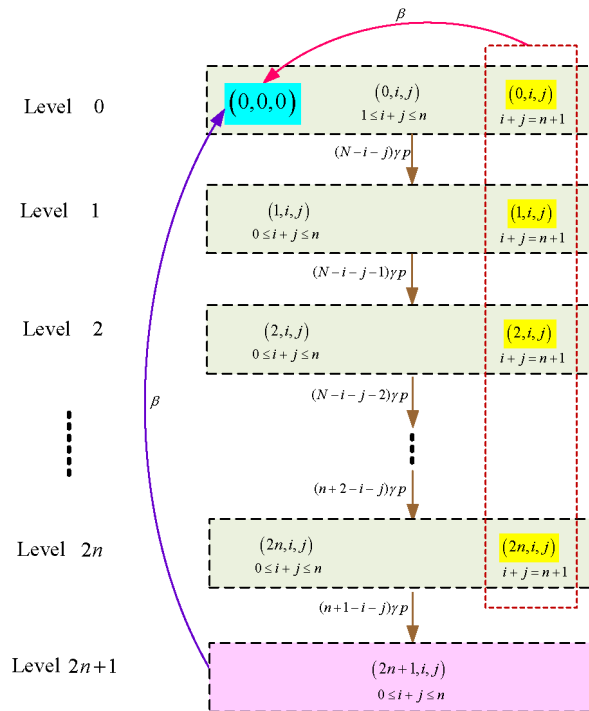


Figure 2: The state transition relations of the Markov process among multiple levels.

Using the Markov process $\{(N(t), M(t), K(t)) : t \geq 0\}$, it is easy to see that the transaction package becomes a block at each of states $(2n + 1, i, j)$ for $0 \leq i, j \leq n$; while the transaction package becomes an orphan block at states (k, i, j) with $0 \leq k \leq 2n$, $0 \leq i, j \leq n + 1$, $i + j = n + 1$. Also, the events that determine a transaction package as either a block or an orphan block are mutually exclusive. Therefore, we can analyze the probability distribution that a transaction package is generated as either a block or an orphan block.

4.1 The block-generated time distribution

To analyze the block-generated time distribution, we set up a new Markov process with an absorption state Δ_1 . To do this, all the states in the set

$$\{(2n + 1, i, j) : 0 \leq i, j \leq n\}$$

are regarded as an absorption state Δ_1 . In this case, the Markov process $\{(N(t), M(t), K(t)) : t \geq 0\}$ operates on a new state space with the absorption state Δ_1 as follows:

$$\{\Delta_1\} \cup \{(k, i, j) : k = 0, 1, 2, \dots, 2n, 0 \leq i + j \leq n\}.$$

At the same time, the state transition relations of the Markov process $\{(N(t), M(t), K(t)) : t \geq 0\}$ with the absorption state Δ_1 are depicted in Figures 3 and 4. Also, its infinitesimal generator is given by

$$\Psi = \begin{pmatrix} 0 & 0 \\ T^0 & T \end{pmatrix},$$

where, $T^0 + T\mathbf{e} = 0$,

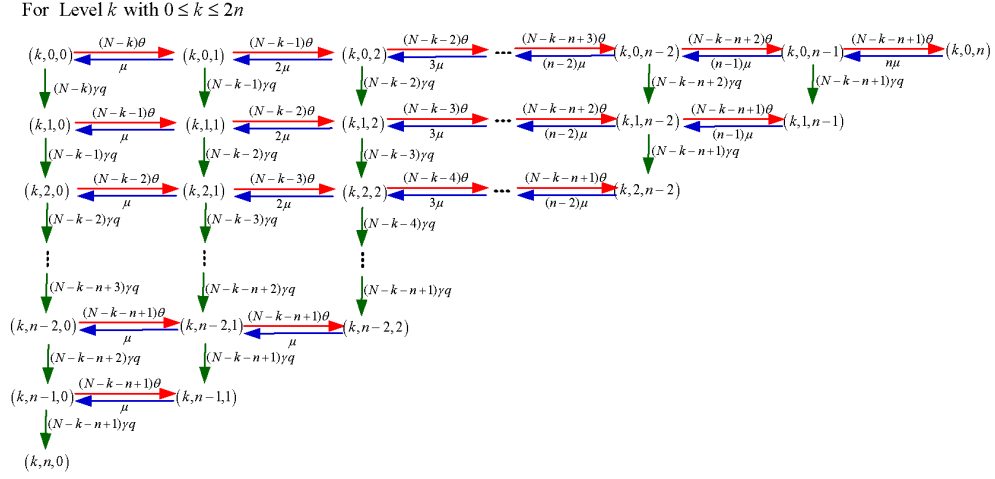


Figure 3: The state transition relations of the Markov process Ψ : Part one.

$$T^0 = \begin{pmatrix} 0 \\ \vdots \\ 0 \\ T_{2n}^0 \end{pmatrix}, T_{2n}^0 = \begin{pmatrix} L_0 \\ L_1 \\ \vdots \\ L_n \end{pmatrix},$$

$$L_i = \begin{pmatrix} (n+1-i)\gamma p \\ (n-i)\gamma p \\ \vdots \\ \gamma p \end{pmatrix}_{(n+1-i) \times 1}, 0 \leq i \leq n;$$

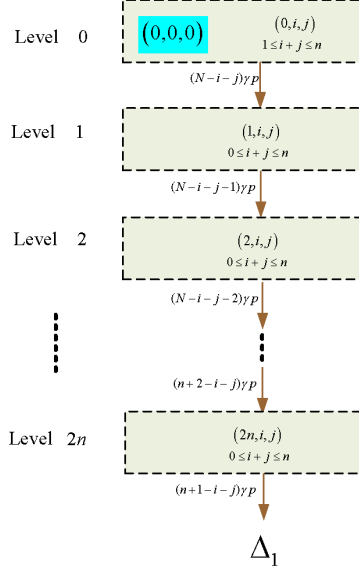


Figure 4: The state transition relations of the Markov process Ψ : Part two.

$$T = \begin{pmatrix} T_{0,0} & T_{0,1} & & & & \\ & T_{1,1} & T_{1,2} & & & \\ & & \ddots & \ddots & & \\ & & & T_{2n-1,2n-1} & T_{2n-1,2n} & \\ & & & & T_{2n,2n} & \end{pmatrix},$$

for $0 \leq k \leq 2n-1$,

$$T_{k,k+1} = \begin{pmatrix} F_{0,0}^{(k)} & & & & \\ & F_{1,1}^{(k)} & & & \\ & & \ddots & & \\ & & & & F_{n,n}^{(k)} \end{pmatrix},$$

for $0 \leq i \leq n$,

$$F_{i,i}^{(k)} = \begin{pmatrix} (N-k-i)\gamma p & & & & \\ & (N-k-i-1)\gamma p & & & \\ & & \ddots & & \\ & & & & (N-k-n)\gamma p \end{pmatrix}_{(n+1-i) \times (n+1-i)} ;$$

for $0 \leq k \leq 2n$,

$$T_{k,k} = \begin{pmatrix} K_{0,0}^{(k)} & K_{0,1}^{(k)} & & & & \\ & K_{1,1}^{(k)} & K_{1,2}^{(k)} & & & \\ & & \ddots & \ddots & & \\ & & & K_{n-1,n-1}^{(k)} & K_{n-1,n}^{(k)} & \\ & & & & & K_{n,n}^{(k)} \end{pmatrix},$$

for $0 \leq i \leq n-1$,

$$K_{i,i+1}^{(k)} = \begin{pmatrix} (N-k-i)\gamma q & & & & & \\ & (N-k-i-1)\gamma q & & & & \\ & & \ddots & & & \\ & & & (N-k-n+1)\gamma q & & \\ & & & & 0 & \end{pmatrix}_{(n+1-i) \times (n-i)},$$

$$K_{i,i}^{(k)} = \begin{pmatrix} c_{k,i,0} & (N-k-i)\theta & & & & \\ \mu & c_{k,i,1} & (N-k-i-1)\theta & & & \\ & \ddots & \ddots & \ddots & & \\ & & (n-i-1)\mu & c_{k,i,n-i-1} & (N-k-n+1)\theta & \\ & & & (n-i)\mu & c_{k,i,n-i} & \end{pmatrix}_{(n+1-i) \times (n+1-i)},$$

$$c_{k,i,m} = -[(N-k-i-m)(\theta + \gamma) + m\mu], 0 \leq m \leq n-i-1,$$

$$c_{k,i,n-i} = -[(N-k-n)\gamma p + (n-i)\mu],$$

$$K_{n,n}^{(k)} = -(N-k-n)\gamma p.$$

Note that the block-generated time W_B of any transaction package at the PBFT-based blockchain system is a time interval from the arrival epoch of the new transaction package to the time when it is determined as a block finally. Here, there is a reason why a transaction package becomes a block. That is, the transaction package obtains enough approval votes, so this transaction package or block can peg to the blockchain.

Let (α_0, α) denote the initial probability distribution of the Markov process Ψ with absorption state Δ_1 at time $t = 0$ for $\alpha_0 = 0$. Then the vector $\alpha = (1, 0, \dots, 0)$ shows that the Markov process T is at the state $(0, 0, 0)$ at time 0. The following theorem provides an expression for the probability distribution of the block-generated time W_B by means of the first passage times and the phase-type distributions of finite sizes.

Theorem 1 *If the initial probability distribution of the Markov process Ψ with absorption state Δ_1 is (α_0, α) for $\alpha_0 = 0$, then the probability distribution of the block-generated time W_B is of phase-type with an irreducible matrix representation (α, T) of finite sizes, and*

$$F_{W_B}(t) = P\{W_B \leq t\} = 1 - \alpha \exp\{Tt\}e, \quad t \geq 0.$$

Also, the average block-generated time is given by

$$E[W_B] = -\alpha T^{-1}e,$$

where T^{-1} is the inverse of the matrix T of finite sizes.

Proof. For $k \in \{0, 1, 2, \dots, 2n\}$, $i \in \{0, 1, 2, \dots, n\}$, $j \in \{0, 1, 2, \dots, n\}$, $0 \leq i + j \leq n$, we write

$$q_{k,i,j}(t) = P\{N(t) = k, J_1(t) = i, J_2(t) = j\},$$

which is the state probability that the QBD process Ψ with absorption state Δ_1 is at state (k, i, j) at time $t \geq 0$ before absorbed to state Δ_1 ,

$$q_k(t) = \{q_{k,0,0}(t), \dots, q_{k,0,n}(t); q_{k,1,0}(t), \dots, q_{k,1,n-1}(t); \dots; q_{k,n,0}(t)\},$$

and

$$q(t) = \{q_0(t), q_1(t), q_2(t), \dots, q_{2n-1}(t), q_{2n}(t)\}.$$

Using the Chapman-Kolmogorov forward differential equation, we can obtain

$$\frac{d}{dt}q(t) = q(t)T, \tag{1}$$

with the initial condition

$$q(0) = \alpha. \tag{2}$$

It follows from (1) and (2) together with $\alpha_0 = 0$ that

$$q(t) = \alpha \exp\{Tt\}. \tag{3}$$

Thus we obtain

$$P\{W_B > t\} = q(t)e = \alpha \exp\{Tt\}e.$$

This gives

$$\begin{aligned} F_{W_B}(t) &= P\{W_B \leq t\} = 1 - P\{W_B > t\} \\ &= 1 - \alpha \exp\{Tt\}e, \quad t \geq 0 \end{aligned}$$

In what follows, we compute the average block-generated time $E[W_B]$. Let $f(s)$ be the Laplace-Stieltjes transform of the distribution function $F_{W_B}(t)$, then

$$f(s) = \int_0^\infty e^{-st} dF_{W_B}(t) = 1 + \alpha(sI - T)^{-1}T^0, \text{ for } s \geq 0,$$

where I denotes an identity matrix of finite size. Hence we obtain that

$$E[W_B] = -\frac{d}{ds}f(s)|_{s=0} = \alpha \left[(sI - T)^{-2} \right]_{|s=0} T^0 = -\alpha T^{-1}e$$

by using $T^0 + T\mathbf{e} = 0$ and $T^{-1}T\mathbf{e} = \mathbf{e}$. This completes the proof. \square

To compute the inverse matrix T^{-1} of finite size, we need to use the RG-factorizations of the Markov process T . To this end, we write

$$T^{-1} = \begin{pmatrix} J_{0,0} & J_{0,1} & J_{0,2} & \cdots & J_{0,2n} \\ & J_{1,1} & J_{1,2} & \cdots & J_{1,2n} \\ & & J_{2,2} & \cdots & J_{2,2n} \\ & & & \ddots & \vdots \\ & & & & J_{2n,2n} \end{pmatrix},$$

By using $T^{-1}T = I$, we can obtain that for $k = 0, 1, \dots, 2n$,

$$J_{k,k} = T_{k,k}^{-1},$$

and for $k = 0, 1, \dots, 2n - 1$, $j = 1, 2, \dots, 2n - k$,

$$J_{k,k+j} = (-1)^j T_{k,k}^{-1} T_{k,k+1} T_{k+1,k+1}^{-1} T_{k+1,k+2} \cdots T_{k+j-1,k+j} T_{k+j,k+j}^{-1}.$$

Therefore, before computing T^{-1} , it is a key to compute the inverse matrices of diagonal block elements $T_{k,k}$ for $k = 0, 1, \dots, 2n$. Note that $K_{i,i}^{(k)} \neq \mathbf{0}$, then the upper triangular matrix $T_{k,k}$ is invertible, and there exists a unique inverse matrix. Thus, we write

$$T_{k,k}^{-1} = \begin{pmatrix} X_{0,0}^{(k)} & X_{0,1}^{(k)} & X_{0,2}^{(k)} & \cdots & X_{0,n}^{(k)} \\ & X_{1,1}^{(k)} & X_{1,2}^{(k)} & \cdots & X_{1,n}^{(k)} \\ & & X_{2,2}^{(k)} & \cdots & X_{2,n}^{(k)} \\ & & & \ddots & \vdots \\ & & & & X_{n,n}^{(k)} \end{pmatrix}, \quad 0 \leq k \leq 2n.$$

By using $T_{k,k} T_{k,k}^{-1} = I$, we can obtain that for $i = 0, 1, \dots, n$,

$$X_{i,i}^{(k)} = \left(K_{i,i}^{(k)} \right)^{-1},$$

and for $i = 0, 1, \dots, n-1, j = 1, 2, \dots, n-i$,

$$X_{i,i+j}^{(k)} = (-1)^j \left(K_{i,i}^{(k)} \right)^{-1} K_{i,i+1}^{(k)} \left(K_{i+1,i+1}^{(k)} \right)^{-1} K_{i+1,i+2}^{(k)} \cdots K_{i+j-1,i+j}^{(k)} \left(K_{i+j,i+j}^{(k)} \right)^{-1}.$$

Therefore, before computing $T_{k,k}^{-1}, 0 \leq k \leq 2n$, it is a key to deal with the inverse matrices of diagonal block elements $K_{i,i}^{(k)}$ with the order $n+1-i$ for $i = 0, 1, \dots, n$. Since $K_{i,i}^{(k)}$ is a birth and death process with finite states, we can use RG-factorizations to compute its inverse matrix. Readers may refer to Chapter 1 of Li [64] for more details.

4.2 The orphan-block-generated time distribution

To analyze the orphan-block-generated time distribution, we set up a new Markov process with an absorption state Δ_2 , where, $\Delta_2 = \{ \tilde{\Delta}_k, 0 \leq k \leq 2n \}$. To do this, all the states in the set

$$\{ (k, i, j) : 0 \leq k \leq 2n, 0 \leq i, j \leq n+1, i+j = n+1 \}$$

are regarded as an absorption state Δ_2 . Then the Markov process $\{ (N(t), M(t), K(t)) : t \geq 0 \}$ operates on a new state space with the absorption state Δ_2 as follows:

$$\{ \Delta_2 \} \cup \{ (k, i, j) : 0 \leq k \leq 2n, 0 \leq i+j \leq n \}.$$

In this case, the state transition relations of the Markov process $\{ (N(t), M(t), K(t)) : t \geq 0 \}$ with the absorption state Δ_2 are depicted in Figures 5 and 6. Also, its infinitesimal generator is given by

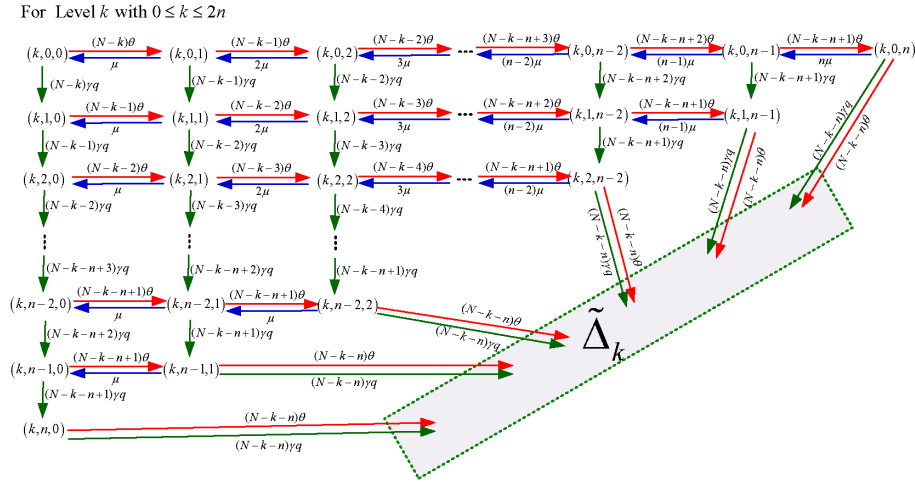


Figure 5: The state transition relations of the Markov process Θ : Part one.

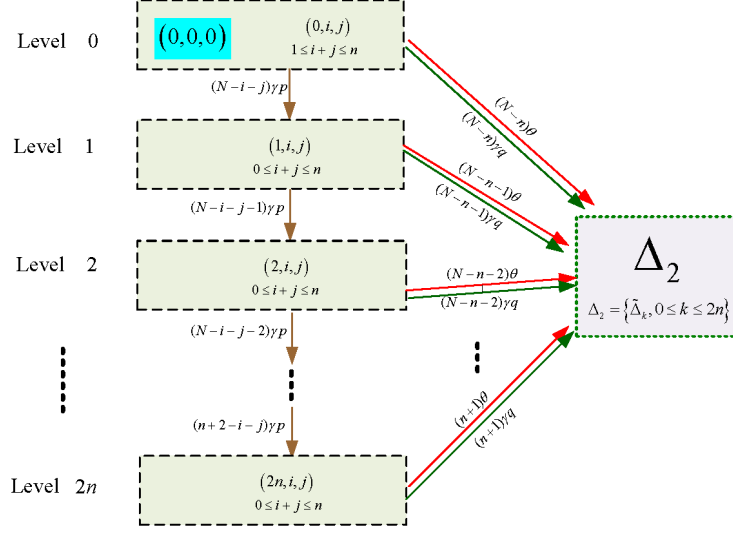


Figure 6: The state transition relations of the Markov process Θ : Part Two.

$$\Theta = \begin{pmatrix} 0 & 0 \\ S^0 & S \end{pmatrix},$$

where $S^0 + S\mathbf{e} = 0$. In order to increase the readability of this paper, the non-zero matrix elements of Θ can be found in the Appendix A.

The orphan-block-generated time W_O of any transaction package at the PBFT-based blockchain system is a time interval from the arrival epoch of a new transaction package to the time when it is determined as an orphan block finally. Here, there is a reason why a transaction package becomes an orphan block. That is, the transaction package cannot obtain enough approval votes, so this transaction package or orphan block needs to roll back to the transaction pool.

Let (ω_0, ω) denote the initial probability distribution of the Markov process Θ with absorption state Δ_2 at time $t = 0$ for $\omega_0 = 0$. Then the vector $\omega = (1, 0, \dots, 0)$ shows that the Markov process S is at the state $(0, 0, 0)$ at time 0.

The following theorem provides an expression for the probability distribution of the orphan-block-generated time W_O by means of the first passage times and the phase-type distributions of finite sizes. The proof is omitted here to save space time since it is similar to that given in Theorem 1.

Theorem 2 *If the initial probability distribution of the Markov process Θ with absorp-*

tion state Δ_2 is (ω_0, ω) for $\omega_0 = 0$, then the probability distribution of the orphan-block-generated time W_O is of phase-type with an irreducible matrix representation (ω, S) of finite sizes, and

$$F_{W_O}(t) = P\{W_O \leq t\} = 1 - \omega \exp\{St\}e, \quad t \geq 0.$$

Also, the average orphan-block-generated time is given by

$$E[W_O] = -\omega S^{-1}e.$$

5 Queueing Analysis for the PBFT-based Blockchain System

In this section, we set up an $M \oplus PH^b/PH^b/1$ queue to study the PBFT-based blockchain system with repairable voting nodes. Based on this, we first give the stationary probability vector of the queueing model for the PBFT-based blockchain system, and then provide performance analysis for the PBFT-based blockchain system with repairable voting nodes.

5.1 An $M \oplus PH^b/PH^b/1$ queue

From the block- and orphan-block-generated processes given in Section 4, we set up an $M \oplus PH^b/PH^b/1$ queue to provide performance analysis for the PBFT-based blockchain systems with repairable voting nodes. To do this, the $M \oplus PH^b/PH^b/1$ queue is described as follows:

(1) Transaction arrivals at the transaction pool: In the PBFT-based blockchain system with repairable voting nodes, the arrival process of transactions contains two parts:

(a) The external transactions arrive at the transaction pool: We assume that the external transactions arrive at the transaction pool according to a Poisson process with an arrival rate $\lambda > 0$.

(b) The orphan blocks are rolled back to the transaction pool: We subdivide the roll-back of every orphan block into two stages: The first stage is to determine the transaction package as an orphan block by the voting nodes; The second stage is to roll back the orphan block to the transaction pool through the network propagation. As seen from Subsection 4.2, the orphan-block-generated time W_O follows a PH distribution with irreducible matrix representation (ω, S) of finite sizes, where the size of the orphan block is

b. In addition, we assume that the rollback time of the orphan block is exponential with the rollback rate β . See Figure 7 for more details.

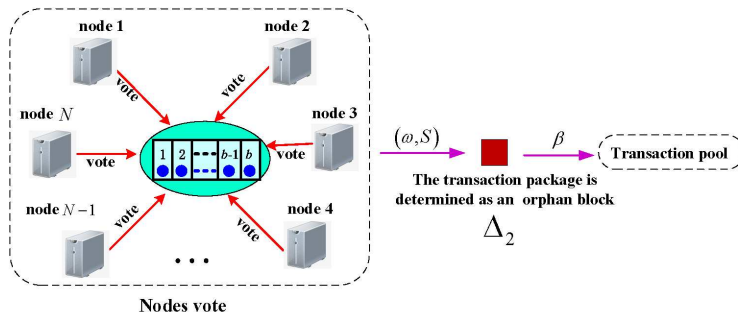


Figure 7: The process that the orphan block is rolled back to the transaction pool.

Combining Assumptions **(a)** with **(b)**, it is seen that the total transaction arrivals at the PBFT-based blockchain system with repairable voting nodes are two processes: One is of phase type with irreducible matrix representation (ω, S) ; while another is Poisson with arrival rate λ .

(2) The service times: We regard the block-generated and block-pegged process as a two-stage service process in the PBFT-based blockchain system with repairable voting nodes, that is, the service process contains two stages: The first stage is that the PBFT-based blockchain system with repairable voting nodes randomly selects b transactions from the transaction pool with equal probability to form a transaction package, and then this transaction package can be successfully determined as a block by the voting nodes; the second stage is that this block is pegged on the blockchain through the network propagation. Referring to Subsection 4.1, the block-generated time W_B of every transaction package at the PBFT-based blockchain system follows a PH distribution with irreducible matrix representation (α, T) of finite sizes, where the size of the orphan block is b . Also, we assume that the block-pegged time of the block in the network follows an exponential distribution with the block-pegged rate β . See Figure 8 for more details.

(3) Independence: We assume that all random variables defined above are independent of each other.

From the above model assumptions, it is easy to see that the PBFT-based blockchain system with repairable nodes can be described as an $M \oplus PH^b / PH^b / 1$ queue, which is depicted in Figure 9. To compute easily, we need to express the service time. Note that a block is pegged to the blockchain through two-stage processes: a PH distribution and an

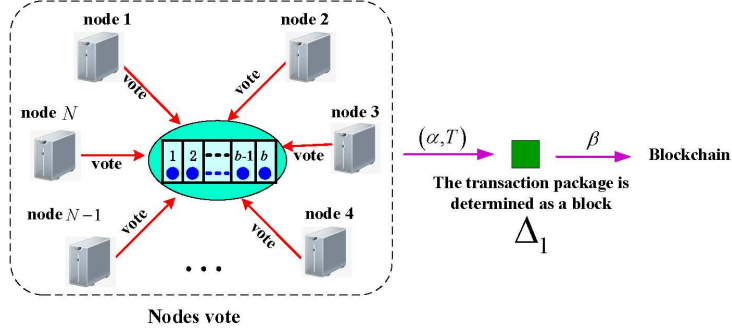


Figure 8: Two different stages that the block enters the blockchain.

exponential distribution, the total time of these two is written as a Markov process whose infinitesimal generator is given by:

$$\begin{pmatrix} T & T^0 & 0 \\ 0 & -\beta & \beta \\ 0 & 0 & 0 \end{pmatrix},$$

where the final state is an absorbing state. Let

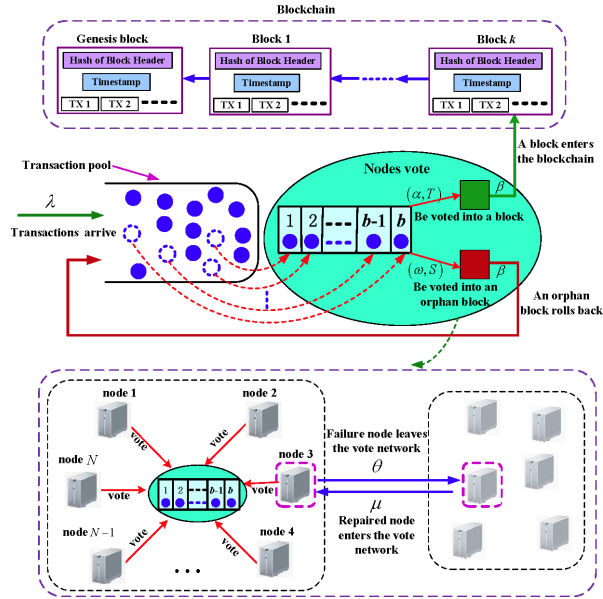


Figure 9: The $M \oplus PH^b / PH^b / 1$ queue.

$$\tilde{T} = \begin{pmatrix} T & T^0 \\ 0 & -\beta \end{pmatrix},$$

$$\tilde{T}^0 = \begin{pmatrix} 0 \\ \beta \end{pmatrix},$$

$$\tilde{\alpha} = (\alpha, 0).$$

It is clear that the time length that the block is generated and pegged to the blockchain follows a continuous-time PH distribution with irreducible matrix representation $(\tilde{\alpha}, \tilde{T})$.

Similarly, the time length that the orphan block is generated and rolled back to the transaction pool follows a continuous-time PH distribution with irreducible matrix representation $(\tilde{\omega}, \tilde{S})$, where,

$$\tilde{S} = \begin{pmatrix} S & S^0 \\ 0 & -\beta \end{pmatrix},$$

$$\tilde{\omega} = (\omega, 0).$$

5.2 Analysis of the $M \oplus PH^b / PH^b / 1$ queue

Let $I(t)$ be the number of transactions in the transactions pool at time t . Then

$$I(t) \in \{0, 1, 2, \dots, b-1, b, b+1, b+2, \dots\}.$$

We denote by $C(t)$ and $D(t)$ the phases of the block-generated time and the orphan-block-generated time at time t , respectively. It is clear that $\{(I(t), C(t), D(t)) : t \geq 0\}$ is a continuous-time Markov Process.

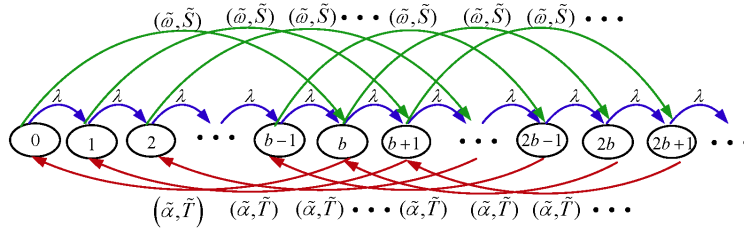


Figure 10: The state transition relations of the Markov process $\{(I(t), C(t), D(t)) : t \geq 0\}$.

Based on Figure 10, the infinitesimal generator Υ of the Markov process $\{(I(t), C(t), D(t)) : t \geq 0\}$ is given by

$$\Upsilon = \begin{pmatrix} B_1^{(0)} & A_0^{(0)} & & & \\ A_2^{(1)} & A_1 & A_0 & & \\ & A_2 & A_1 & A_0 & \\ & & \ddots & \ddots & \ddots \end{pmatrix},$$

where

$$B_1^{(0)} = \begin{pmatrix} \tilde{S} - \lambda I & \lambda I & & & \\ & \tilde{S} - \lambda I & \lambda I & & \\ & & \ddots & \ddots & \\ & & & \tilde{S} - \lambda I & \lambda I \\ & & & & \tilde{S} - \lambda I \end{pmatrix},$$

$$A_0^{(0)} = \begin{pmatrix} (\tilde{S}^0 \tilde{\omega}) \otimes \tilde{\alpha} & & & & \\ & (\tilde{S}^0 \tilde{\omega}) \otimes \tilde{\alpha} & & & \\ & & \ddots & & \\ \lambda(I \otimes \tilde{\alpha}) & & & & (\tilde{S}^0 \tilde{\omega}) \otimes \tilde{\alpha} \end{pmatrix},$$

$$A_2^{(1)} = \begin{pmatrix} I \otimes \tilde{T}^0 & & & & \\ & I \otimes \tilde{T}^0 & & & \\ & & \ddots & & \\ & & & I \otimes \tilde{T}^0 & \end{pmatrix},$$

$$A_2 = \begin{pmatrix} I \otimes (\tilde{T}^0 \tilde{\alpha}) & & & & \\ & I \otimes (\tilde{T}^0 \tilde{\alpha}) & & & \\ & & \ddots & & \\ & & & I \otimes (\tilde{T}^0 \tilde{\alpha}) & \end{pmatrix},$$

$$A_1 = \begin{pmatrix} \tilde{S} \oplus \tilde{T} - \lambda I & \lambda I & & & \\ & \tilde{S} \oplus \tilde{T} - \lambda I & \lambda I & & \\ & & \ddots & \ddots & \\ & & & \tilde{S} \oplus \tilde{T} - \lambda I & \lambda I \\ & & & & \tilde{S} \oplus \tilde{T} - \lambda I \end{pmatrix},$$

$$A_0 = \begin{pmatrix} (\tilde{S}^0 \tilde{\omega}) \otimes I & & & \\ & (\tilde{S}^0 \tilde{\omega}) \otimes I & & \\ & & \ddots & \\ \lambda I & & & (\tilde{S}^0 \tilde{\omega}) \otimes I \end{pmatrix},$$

and I is the identity matrix of appropriate dimensions.

Obviously, the continuous-time Markov process Υ is a level-independent QBD process. Thus, we can apply the matrix-geometric solution given in Neuts [63] to analyze the QBD process Υ . Based on this, we can further analyze the PBFT-based blockchain system with repairable voting nodes.

Theorem 3 *The level-independent QBD Υ is positive recurrent if and only if*

$$\lambda + b\delta_1 \tilde{S}^0 < b\delta_2 \tilde{T}^0,$$

where δ_1 and δ_2 are the stationary probability vectors of the two Markov processes $\tilde{T} + \tilde{T}^0 \tilde{\alpha}$ and $\tilde{S} + \tilde{S}^0 \tilde{\omega}$, respectively.

Proof. Let $W = (\tilde{S} + \tilde{S}^0 \tilde{\omega}) \oplus (\tilde{T} + \tilde{T}^0 \tilde{\alpha})$. Since δ_1 satisfies $\delta_1(\tilde{T} + \tilde{T}^0 \tilde{\alpha}) = 0$, $\delta_1 e = 1$; and δ_2 satisfies $\delta_2(\tilde{S} + \tilde{S}^0 \tilde{\omega}) = 0$, $\delta_2 e = 1$. It is easy to see that $(\delta_1 \otimes \delta_2) \left[(\tilde{S} + \tilde{S}^0 \tilde{\omega}) \oplus (\tilde{T} + \tilde{T}^0 \tilde{\alpha}) \right] = 0$.

For the continuous-time QBD process Υ , we use the mean-drift method to provide its stability condition. Readers may refer to Chapter 1 of Neuts [63] or Chapter 3 of Li [64] for more details. We write

$$A = A_2 + A_1 + A_0 = \begin{pmatrix} W - \lambda I & \lambda I & & & \\ & W - \lambda I & \lambda I & & \\ & & \ddots & \ddots & \\ & & & W - \lambda I & \lambda I \\ \lambda I & & & & W - \lambda I \end{pmatrix},$$

Clearly, the Markov process A is irreducible, aperiodic and positive recurrent. Let $v = (v_1, v_2, \dots, v_b)$ be the stationary probability vector of Markov process A , where $v_k = \gamma_k(\delta_1 \otimes \delta_2)$, $k = 1, 2, \dots, b$. Then from the system of linear equations: $vA = 0$ and $ve = 1$, we easily get that $\gamma_1 = \gamma_2 = \dots = \gamma_b = 1/b$, thus, we obtain $v_k = (\delta_1 \otimes \delta_2)/b$, $k = 1, 2, \dots, b$.

Using the mean-drift method, it is easy to check that the QBD process Υ is positive recurrent if and only if $vA_0e < vA_2e$, i.e.,

$$\lambda + b\delta_1\tilde{S}^0 < b\delta_2\tilde{T}^0.$$

This completes the proof. \square

When the QBD process Υ is positive recurrent, we write its stationary probability vector as $\psi = (\psi_0, \psi_1, \psi_2, \dots)$, where

$$\psi_k = \left(\tilde{\psi}_{kb}, \tilde{\psi}_{kb+1}, \dots, \tilde{\psi}_{(k+1)b-1} \right), k \geq 0.$$

Note that such a stationary probability vector ψ in general has no explicit expression, we can only develop its numerical solution. To this end, by using the Chapter 3 in Neuts [63], we need to numerically compute the rate matrix R , which is the minimal nonnegative solution to the nonlinear matrix equation $R^2A_2 + RA_1 + A_0 = 0$. Based on this, we give an iterative algorithm (see Chapter 3 of Neuts [63]) to numerically compute the rate matrix R as follows:

$$\begin{aligned} R_0 &= 0, \\ R_{n+1} &= (R_n^2A_2 + A_0)(-A_1^{-1}), n = 1, 2, 3, \dots \end{aligned} \quad (4)$$

For the matrix sequence $\{R_n, n \geq 0\}$, by means of Chapter 3 in Neuts [63], it is easy to see that as $n \rightarrow \infty$, $R_n \uparrow R$. Thus, for any sufficiently small positive number ε , there exists a positive integer \mathbf{n} such that $\|R_{\mathbf{n}+1} - R_{\mathbf{n}}\| < \varepsilon$. In this case, we take $R \approx R_{\mathbf{n}}$, which gives an approximate solution to the nonlinear matrix equation $R^2A_2 + RA_1 + A_0 = 0$.

Using the rate matrix R , the following theorem provides an expression for the stationary probability vector ψ . This conclusion is directly derived from Theorem 1.2.1 of Chapter 1 of Neuts [63]. Here, we restate it without a proof.

Theorem 4 *If the QBD process Υ is positive recurrent, then its stationary probability vector $\psi = (\psi_0, \psi_1, \psi_2, \dots)$ is given by*

$$\psi_k = \psi_1 R^{k-1}, k \geq 1, \quad (5)$$

where ψ_0 and ψ_1 are the unique solution to the following system of linear equations:

$$\begin{cases} \psi_0 B_1^{(0)} + \psi_1 A_2^{(1)} = 0, \\ \psi_0 A_0^{(0)} + \psi_1 (A_1 + RA_2) = 0, \\ \psi_0 e + \psi_1 (I - R)^{-1} e = 1. \end{cases} \quad (6)$$

5.3 Performance measures of the PBFT system

Based on the $M \oplus PH^b/PH^b/1$ queue and the stationary probability vector ψ , we can provide some key performance measures of the PBFT-based blockchain system with repairable voting nodes as follows:

(a1) The stationary probability of no transaction package in the PBFT-based blockchain system is given by

$$\eta_1 = \psi_0 e.$$

(a2) The stationary probability of existing transaction package in the PBFT-based blockchain system is given by

$$\eta_2 = 1 - \eta_1 = 1 - \psi_0 e.$$

(b1) The stationary rate that a block is pegged on the blockchain in the PBFT-based blockchain system is given by

$$r_1 = (1 - \psi_0 e) \frac{1}{(-\tilde{\alpha}\tilde{T}^{-1}e)} = \eta_2 \frac{1}{(-\tilde{\alpha}\tilde{T}^{-1}e)}.$$

(b2) The stationary rate that an orphan block is rolled back to the transaction pool is given by

$$r_2 = (1 - \psi_0 e) \frac{1}{(-\tilde{\omega}\tilde{S}^{-1}e)} = \eta_2 \frac{1}{(-\tilde{\omega}\tilde{S}^{-1}e)}.$$

(c) The block throughput of the PBFT-based blockchain system is given by

$$\text{TH}(\text{block}) = (1 - \psi_0 e) \frac{1}{(-\tilde{\alpha}\tilde{T}^{-1}e)} = \eta_2 \frac{1}{(-\tilde{\alpha}\tilde{T}^{-1}e)}.$$

In this paper, we define the block throughput as the number of blocks per second, and transaction throughput as the number of transactions per second. The latter is a common and general definition of throughput and the focus of our attention.

In what follows, we provide an effective method to compute the transaction throughput of the PBFT-based blockchain system with repairable voting nodes.

Theorem 5 *The transaction throughput of the PBFT-based blockchain system is given by*

$$\text{TH} = (1 - \psi_0 e) \frac{b}{(-\tilde{\alpha}\tilde{T}^{-1}e)} = \eta_2 \frac{b}{(-\tilde{\alpha}\tilde{T}^{-1}e)}.$$

Proof. We only consider the transaction throughput TH. From Theorem 1 in Subsection 4.1, it is seen that the block-generated time W_B of any transaction package in the PBFT-based blockchain system follows a PH distribution with irreducible matrix representation $(\tilde{\alpha}, \tilde{T})$. This gives that the average time that the PBFT-based blockchain system pegs a block with b transactions on the blockchain is $(-\tilde{\alpha}\tilde{T}^{-1}e)$. Therefore, the number of transactions dealt with by the PBFT-based blockchain system per unit time is $b/(-\tilde{\alpha}\tilde{T}^{-1}e)$.

In addition, the stationary probability of the existing transaction package in the PBFT-based blockchain system is given by η_2 . Thus, the transaction throughput of the PBFT-based blockchain system is the product of the stationary probability of the existing transaction package in the PBFT-based blockchain system and the number of transactions dealt with per unit time in the PBFT-based blockchain system, thus, we obtain

$$\text{TH} = (1 - \psi_0 e) \frac{b}{(-\tilde{\alpha}\tilde{T}^{-1}e)} = \eta_2 \frac{b}{(-\tilde{\alpha}\tilde{T}^{-1}e)}.$$

This completes the proof. \square

6 Reliability Analysis of the PBFT-based Blockchain System

In this section, we set up two new Markov processes to analyze the reliability of the PBFT-based blockchain system with repairable voting nodes. Here, our purpose focuses on such a condition: is considered to be the inability of the blockchain system to produce any blocks. In what follows, we consider two different cases.

6.1 Unavailability due to failed nodes

In this subsection, we consider the case where the PBFT-based blockchain system becomes unavailable due to the number of failed nodes reaching $n+1$. In this case, the PBFT-based blockchain system can no longer carry out the voting process such that no new blocks are generated.

Note that every node may fail and need to be repaired, with the failure rate of θ and the repair rate of μ . Let $K(t)$ represent the number of failed nodes in the PBFT-based blockchain system at time t , then $\{K(t), t \geq 0\}$ is a continuous-time birth-death process,

To analyze the inherent reliability $R_1(t)$ of the PBFT-based blockchain system with repairable voting nodes, we let all the states in the set $\{n+1, n+2, \dots, N\}$ be absorption state ∇_1 . Then the Markov process $\{K(t), t \geq 0\}$ operates on a new state space $\{0, 1, 2, \dots, n\} \cup \{\nabla_1\}$, and its state transition relations are depicted in Figure 12.

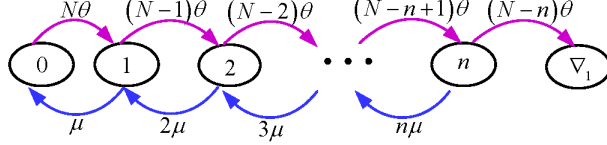


Figure 12: The state transition relations of the Markov process $\{K(t), t \geq 0\}$ with the absorption state ∇_1 .

We write

$$Q_{\nabla_1} = \begin{pmatrix} T_{\nabla} & T_{\nabla}^0 \\ 0 & 0 \end{pmatrix},$$

where,

$$T_{\nabla} = \begin{pmatrix} -N\theta & N\theta & & & & \\ \mu & -[\mu + (N-1)\theta] & (N-1)\theta & & & \\ & \ddots & \ddots & \ddots & & \\ & & (n-1)\mu & -[(n-1)\mu + (N-n+1)\theta] & (N-n+1)\theta & \\ & & & n\mu & -[n\mu + (N-n)\theta] & \end{pmatrix},$$

$$T_{\nabla}^0 = \begin{pmatrix} 0 \\ \vdots \\ 0 \\ (N-n)\theta \end{pmatrix}.$$

Let $(\varphi(0), \varphi_0(0))$ be the initial probability distribution of the Markov process Q_{∇_1} , where $\varphi_0(0) = 0$, and $\varphi(0) = (1, 0, 0, \dots, 0)$, $\tau_1 = \inf \{t \geq 0 : \tilde{K}(t) = n+1, \tilde{K}(0) = 0\}$, and $R_1(t) = P\{\tau_1 > t\}$, then following theorem provides an expression for the inherent reliability $R_1(t)$ of the PBFT-based blockchain system.

Theorem 6 *If the initial probability distribution of the Markov process Q_{∇_1} is $(\varphi(0), \varphi_0(0))$, then the inherent reliability $R_1(t)$ of the PBFT-based blockchain system is given by*

$$R_1(t) = \sum_{k=0}^n \varphi_k(t) \quad (7)$$

and $\varphi(t) = (\varphi_0(t), \varphi_1(t), \dots, \varphi_n(t))$ satisfy the Chapman-Kolmogorov forward differential equation

$$\varphi'(t) = \varphi(t)T_{\nabla} \quad (8)$$

with $(\varphi(0), \varphi_0(0)) = (1, 0, 0, \dots, 0)$.

Proof. It is easy to see that $R_1(t) = \varphi(t)e$. Let

$$\varphi^*(s) = \int_0^{\infty} e^{-st} \varphi(t) dt, \quad s > 0, \quad i = 0, 1, 2, \dots, n,$$

be the Laplace transform of $\varphi(t)$, then

$$\int_0^{\infty} e^{-st} \varphi'(t) dt = \int_0^{\infty} e^{-st} \varphi(t) dt \cdot T_{\nabla}, \quad s > 0,$$

thus, we obtain

$$\varphi^*(s) = \int_0^{\infty} e^{-st} \varphi(t) dt = \varphi(0)(sI - T_{\nabla})^{-1}, \quad s > 0.$$

Also, we have

$$R_1^*(s) = \varphi^*(s)e = \varphi(0)(sI - T_{\nabla})^{-1}e, \quad s > 0.$$

Therefore,

$$R_1(t) = P\{\tau_1 > t\} = \sum_{k=0}^n \varphi_k(t).$$

This completes the proof. \square

Based on Theorem 6, the average time before the first failure of the PBFT-based blockchain system is given by

$$\text{MTTFF}_1 = \int_0^{\infty} R_1(t) dt = R_1^*(0) = -\varphi(0)T_{\nabla}^{-1}e.$$

6.2 Unavailability due to both failed nodes and disapproval votes

In this subsection, we consider the case where the PBFT-based blockchain system becomes unavailable due to the sum of failed nodes and disapproval votes reaching $n + 1$. To this end, we use a three-dimension Markov process to analyze the reliability of the PBFT voting process with repairable voting nodes.

Theorem 7 *The stationary probability vector $\boldsymbol{\pi} = (\pi_0, \pi_1, \pi_2, \dots, \pi_{2n}, \pi_{2n+1})$ of the Markov process Q is matrix-product, and it is given by*

$$\boldsymbol{\pi}_{k+1} = \boldsymbol{\pi}_0 R_0 R_1 \cdots R_k, \quad 0 \leq k \leq 2n, \quad (10)$$

where $\boldsymbol{\pi}_0$ is uniquely determined by means of solving the following system of linear equations

$$\boldsymbol{\pi}_0 (Q_{0,0} + R_0 Q_{1,0} + R_0 R_1 Q_{2,0} + \cdots + R_0 R_1 \cdots R_{2n} Q_{2n+1,0}) = 0 \quad (11)$$

with the normalized condition

$$\boldsymbol{\pi}_0 = 1 / \left(e + \sum_{k=0}^{2n} R_0 R_1 \cdots R_k e \right). \quad (12)$$

Proof. From $\boldsymbol{\pi}Q = 0$ and $\boldsymbol{\pi}e = 1$, we can obtain

$$\begin{cases} \boldsymbol{\pi}_k Q_{k,k+1} + \boldsymbol{\pi}_{k+1} Q_{k+1,k+1} = 0, & 0 \leq k \leq 2n, \\ \sum_{k=0}^{2n+1} \boldsymbol{\pi}_k Q_{k,0} = 0, \\ \sum_{k=0}^{2n+1} \boldsymbol{\pi}_k e = 1. \end{cases} \quad (13)$$

Using (13), we obtain

$$\begin{aligned} \boldsymbol{\pi}_1 &= \boldsymbol{\pi}_0 Q_{0,1} \left(-Q_{1,1}^{-1} \right) = \boldsymbol{\pi}_0 R_0, \\ \boldsymbol{\pi}_2 &= \boldsymbol{\pi}_1 Q_{1,2} \left(-Q_{2,2}^{-1} \right) = \boldsymbol{\pi}_1 R_1 = \boldsymbol{\pi}_0 R_0 R_1, \\ &\vdots \\ \boldsymbol{\pi}_{2n+1} &= \boldsymbol{\pi}_{2n} Q_{2n,2n+1} \left(-Q_{2n+1,2n+1}^{-1} \right) = \boldsymbol{\pi}_{2n} R_{2n} = \boldsymbol{\pi}_0 R_0 R_1 \cdots R_{2n}. \end{aligned}$$

Therefore, we obtain

$$\boldsymbol{\pi}_{k+1} = \boldsymbol{\pi}_0 R_0 R_1 \cdots R_k, \quad 0 \leq k \leq 2n.$$

Further, using equations (10) and (13), we can obtain the boundary equation (11) and the normalized condition (12). This proof is completed. \square

Using the stationary probability vector $\boldsymbol{\pi}$, we can provide reliability analysis of the PBFT-based blockchain system with repairable voting nodes as follows:

(a) The inherent stationary availability of the PBFT-based blockchain system with repairable voting nodes is given by

$$A_2 = 1 - (\pi_{0,0,n+1} + \pi_{1,0,n+1} + \cdots + \pi_{2n,0,n+1}) = 1 - \sum_{k=0}^{2n} \pi_{k,0,n+1}.$$

(b) **The operational stationary availability of the PBFT-based blockchain system with repairable voting nodes** is given by

$$A_3 = 1 - P_O,$$

where P_O represents the stationary probability that the transaction package becomes an orphan block, thus we have

$$P_O = \sum_{k=0}^{2n} \sum_{i=0}^{n+1} \sum_{j=n+1-i} \pi_{k,i,j}.$$

Finally, we provide expression for the operational reliability $R_2(t)$ of the PBFT-based blockchain system. To this end, let all the states in the set

$$\{(0, 0, n+1), (0, 1, n), \dots, (2n, n+1, 0)\}$$

be absorption state ∇_2 . Then the Markov process $\{(N(t), M(t), K(t)) : t \geq 0\}$ operates on a new state space $\Omega_{\nabla} \cup \{\nabla_2\}$, where,

$$\Omega_{\nabla} = \bigcup_{k=0}^{2n+1} \text{Level } k,$$

for $0 \leq k \leq 2n+1$,

$$\begin{aligned} \text{Level } k = & \{(k, 0, 0), (k, 0, 1), \dots, (k, 0, n-2), (k, 0, n-1), (k, 0, n)\}; \\ & (k, 1, 0), (k, 1, 1), \dots, (k, 1, n-2), (k, 1, n-1); \\ & (k, 2, 0), (k, 2, 1), \dots, (k, 2, n-2); \dots; \\ & (k, n, 0)\}. \end{aligned}$$

We write the infinitesimal generator of the the Markov process $\{(N(t), M(t), K(t)) : t \geq 0\}$ with the absorption state ∇_2 as

$$Q_{\nabla_2} = \begin{pmatrix} S_{\nabla} & S_{\nabla}^0 \\ 0 & 0 \end{pmatrix}.$$

Let $(\phi(0), \phi_0(0))$ be the initial probability distribution of the Markov process Q_{∇_2} for $\phi_0(0) = 0$ and $\phi(0) = (1, 0, 0, \dots, 0)$,

$$\tau_2 = \inf \{t \geq 0 : M(t) + K(t) = n+1, (N(0), M(0), K(0)) = (0, 0, 0)\},$$

and $R_2(t) = P\{\tau_2 > t\}$, then following theorem provides expression for the operational reliability $R_2(t)$ of the PBFT-based blockchain system.

Theorem 8 *If the initial probability distribution of the Markov process Q_{∇_2} is $(\phi(0), \phi_0(0))$, then the operational reliability $R_2(t)$ of the PBFT-based blockchain system is given by*

$$R_2(t) = P\{\tau_2 > t\} = \sum_{k=0}^{2n+1} \phi_k(t),$$

where $\phi(t) = (\phi_0(t), \phi_1(t), \dots, \phi_{2n+1}(t))$ satisfy the Chapman-Kolmogorov forward differential equation

$$\phi'(t) = \phi(t)S_{\nabla},$$

and

$$\phi(t) = \phi(0) \exp\{S_{\nabla}t\},$$

where $(\phi(0), \phi_0(0)) = (1, 0, 0, \dots, 0)$.

Based on Theorem 8, the average time before the first failure of the PBFT-based blockchain system is

$$\text{MTTFF}_2 = \int_0^{\infty} R_2(t)dt = -\phi(0)S_{\nabla}^{-1}e.$$

7 Numerical Analysis

In this section, we first provide an efficient algorithm for computing the transaction throughput of the PBFT-based blockchain system with repairable voting nodes. Then we use two groups of numerical examples to verify the validity of our theoretical results and to show how some key system parameters influence performance measures of the PBFT-based blockchain system.

Group One: The impact of important parameters on transaction throughput TH

Before exploring the impact of some important parameters on the transaction throughput of the PBFT-based blockchain system with repairable voting nodes, it is necessary and useful to provide an approximate algorithm, Algorithm 1, to calculate the transaction throughput, which plays an important role in our numerical examples.

Next, we use numerical examples to show the impact of some parameters on the transaction throughput of the PBFT-based blockchain system with repairable voting nodes.

Firstly, we explore the impact of λ and b on TH by means of Algorithm 1. To this end, we take the parameters as follows: $\beta = 0.2$, $\gamma = 0.5$, $\theta = 0.1$, $\mu = 0.2$, $n = 25$, $p = 0.7$, $b \in$

Algorithm 1: Approximately computing transaction throughput TH

Input: The key parameters: $\mu, \theta, \gamma, \beta, p, \lambda, b, n$;

A controllable accuracy ε

Output: Transaction throughput TH of the PBFT-based blockchain system

- 1 Determine transition blocks: \tilde{T}, \tilde{S} and initial probability vectors: $\tilde{\alpha}, \tilde{\omega}$;
- 2 Compute the average rates by using $r_B = 1/(-\tilde{\alpha}\tilde{T}^{-1}e)$ and $r_O = 1/(-\tilde{\omega}\tilde{S}^{-1}e)$;
- 3 Based on the obtained rates r_B and r_O , determine the transition blocks of the QBD process

$$\left\{ B_1^{(0)}, A_2^{(1)}, A_0^{(0)}, A_2, A_1, A_0 \right\};$$

- 4 Use equation (4) to compute the rate matrix R , stop the iteration if

$$\|R_{\mathbf{n}+1} - R_{\mathbf{n}}\| < \varepsilon,$$

and let $R \approx R_{\mathbf{n}}$;

- 5 Solve ψ_0 and ψ_1 by the system equations (6) ;
 - 6 Compute η_2 by equation $\eta_2 = 1 - \psi_0 e$;
 - 7 Compute the transaction throughput TH by equation $\text{TH} = b\eta_2 r_B$;
 - 8 Output the transaction throughput TH.
-

[100, 300], and $\lambda = 0.005, 0.1, 3$. From Fig. 13, we can see that TH increases as b increases, which indicates that the larger the batch size b is, the greater the transaction throughput TH of the PBFT-based blockchain system is. In addition, we can observe that TH increases as λ increases. This indicates that as λ increases, more and more external transactions arrive at the PBFT-based blockchain system, such that the transaction throughput TH of the PBFT-based blockchain system becomes bigger accordingly. Such numerical results are consistent with our intuitive understanding.

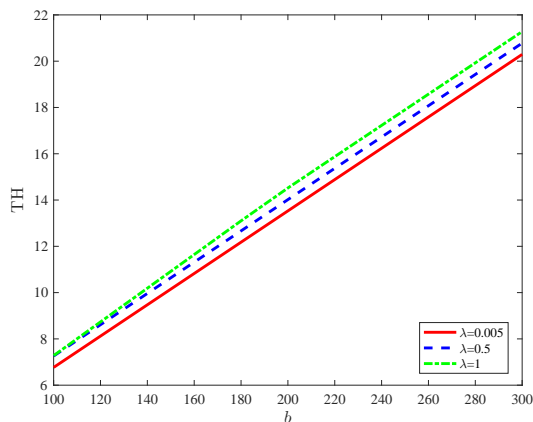


Figure 13: TH vs. b and λ .

Secondly, we explore the impact of μ and p on TH by means of Algorithm 1. To this end, we take the parameters as follows: $\beta = 3$, $\gamma = 5$, $\lambda = 2$, $\theta = 2$, $n = 25$, $b = 100$, $p \in [0.4, 0.725]$, and $\mu = 1.5, 2, 3$. From Fig. 14, we can see that TH increases as p increases, which shows that the higher probability of each voting node approving a transaction package, the greater the transaction throughput of the PBFT-based blockchain system is. In addition, we can see that there exists a p_0 , and when $p < p_0$, the TH decreases as μ increases; when $p > p_0$, the TH increases as μ increases. This result indicates that as μ increases, more and more repaired nodes enter the network, which increases the probability that the PBFT-based blockchain system finds the judgment condition of the voting process. However, the smaller p can increase the chance of determining a transaction package as an orphan block and then decrease the transaction throughput; While the larger p can increase the chance of determining a transaction package as a block, thereby increasing the transaction throughput. Such numerical results are consistent with our intuitive understanding.

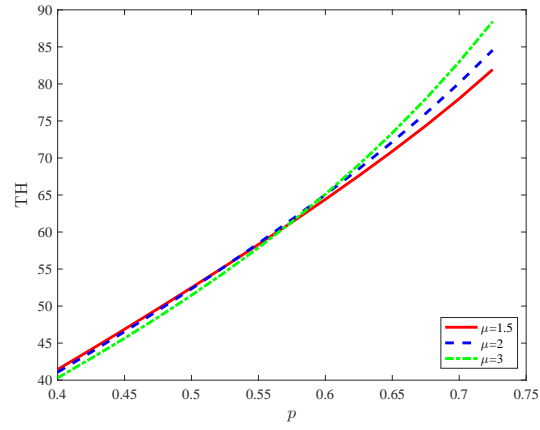


Figure 14: TH vs. p and μ .

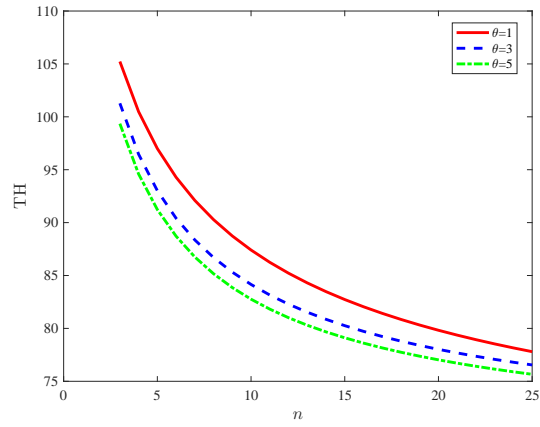


Figure 15: TH vs. n and θ .

Finally, we explore the impact of θ and n on TH by means of Algorithm 1. To this end, we take the parameters as follows: $\beta = 3$, $\gamma = 5$, $\lambda = 2$, $\mu = 2$, $p = 0.68$, $b = 100$, $n \in [3, 25]$, and $\theta = 1, 3, 5$. From Fig. 15, we observe that TH decreases as n increases, which indicates that the increase of n decreases the probability that the PBFT-based blockchain system arrives at the judgment condition, such that the transaction throughput TH decreases. That is, if we aim to pursue the high transaction throughput of a PBFT-based blockchain system, we need a smaller number of total voting nodes. However, if the majority of these nodes are Byzantine, the security of the PBFT-based blockchain system may be compromised. This fact means that we sometimes have to sacrifice the throughput to secure the PBFT-based blockchain system. In addition, we can see that the transaction throughput TH decreases as θ increases. This result indicates that as θ increases, more and more failed nodes leave the PBFT-based blockchain system, which can decrease the probability that the PBFT-based blockchain system arrives at the judgment condition, such that the transaction throughput TH decreases. Such numerical results are also consistent with our intuitive understanding.

In what follows, Table 1 shows the orders of some important sub-matrices with different b and n . It can be seen that the orders of sub-matrices expand rapidly under the influence of the Kronecker operators and n . Such sub-matrices with higher order limit the ability to calculate the transaction throughput TH. Therefore, our approximate algorithm provides an effective and convenient method to calculate transaction throughput, so this approximate algorithm has more general applicability and universality to the study of PBFT-based blockchain systems.

Table 1: The orders of important sub-matrices with different b and n

values of n	\tilde{S} or \tilde{T}	$\tilde{S} \oplus \tilde{T} - \lambda I$	A_1
2	31×31	961×961	$961b \times 961b$
3	71×71	5041×5041	$5041b \times 5041b$
4	136×136	18496×18496	$18496b \times 18496b$
5	231×231	53361×53361	$53361b \times 53361b$

Group Two: The impact of important parameters on the availabilities

In this part, we explore the impact of the parameters n , μ and θ on the availabilities A_1 and A_2 . For Fig. 16(a), we take the parameters as follows: $\theta = 0.5$, $n \in [3, 25]$ and

$\mu = 1.5, 2, 2.5$; For Fig. 16(b), we take the parameters as follows: $\mu = 1.5$, $n \in [3, 25]$, and $\theta = 0.3, 0.35, 0.4$; For Fig. 17(a), we take the parameters as follows: $\beta = 3$, $\theta = 2$, $\gamma = 10$, $p = 0.7$, $n \in [3, 25]$ and $\mu = 1.5, 2, 3$; For Fig. 17(b), we take the parameters as follows: $\beta = 3$, $\mu = 2$, $\gamma = 10$, $p = 0.7$, $n \in [3, 25]$, and $\theta = 1, 2, 3$.

From Fig. 16 and Fig. 17, we can see that the stationary availabilities A_1 and A_2 increase as n increases, which indicates that the total voting nodes $N = 3n + 1$ of the PBFT-based blockchain system with repairable voting nodes can increase the stationary availabilities A_1 and A_2 . In other words, the more voting nodes, the higher the stationary availability of the PBFT-based blockchain system is. Also, it can be seen from Fig. 16 and Fig. 17 that when n increases to a certain value, the increase of the stationary availability A_1 or A_2 is no longer obvious. On the other hand, Fig. 16(a) and Fig. 17(a) show that the stationary availability A_1 (or A_2) increases as μ increases and indicate that the stationary availability A_1 (or A_2) decreases as θ increases. These numerical results indicate that when the total number of nodes $N = 3n + 1$ is constant, more and more repaired nodes enter the PBFT-based blockchain system as μ increases, which can increase the stationary availability A_1 (or A_2). Instead, more and more failed nodes leave the PBFT-based blockchain system as θ increases, which can decrease the stationary availability A_1 (or A_2). Such numerical results are consistent with our intuitive understanding.

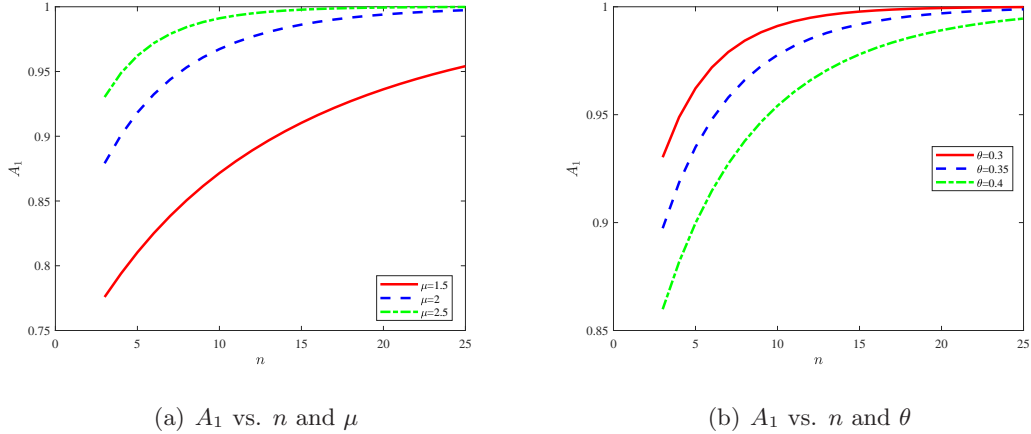
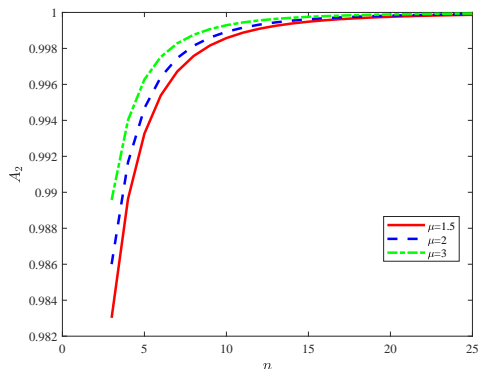
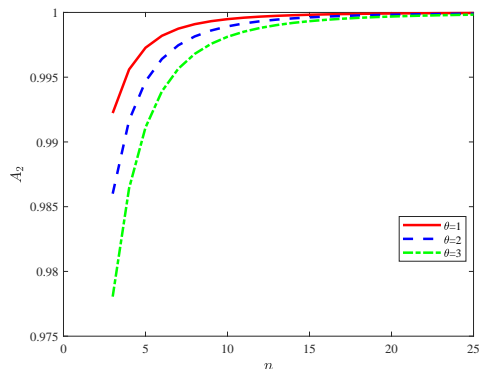


Figure 16: A_1 vs. three parameters n , μ and θ .

Finally, from Groups One and Two of the numerical examples, we can observe that when the total number of voting nodes is constant, the number of voting nodes in the PBFT-based blockchain system affects the throughput, security, and reliability of the



(a) A_2 vs. n and μ



(b) A_2 vs. n and θ

Figure 17: A_2 vs. three parameters n , μ and θ .

PBFT-based blockchain system. That is, the greater the number of voting nodes is, the higher the availability and security of the PBFT-based blockchain system are, but the lower the throughput is. This result shows again that high throughput, high security, and high availability do not coexist. In this case, we sometimes have to sacrifice the throughput to ensure the security and availability of the PBFT-based blockchain system.

8 Concluding Remarks

In this paper, we propose a new PBFT to generalize the ordinary PBFT by introducing a process in which the voting nodes in the PBFT-based blockchain system can fail and be repaired. Specifically, the voting nodes in the new PBFT-based blockchain system may leave the PBFT network while some repaired nodes can re-enter the PBFT network again. In this case, the number of working voting nodes in the new PBFT-based blockchain system is variable, but the total number of voting nodes must be constant. For this PBFT-based blockchain system with repairable voting nodes, we provide a large-scale Markov modeling method to analyze the PBFT-based blockchain system. Also, we provide performance analysis for the PBFT-based blockchain system with repairable voting nodes. At the same time, we perform a reliability analysis for the PBFT-based blockchain system with repairable voting nodes and propose some reliability measures, including availability, reliability, and the average time before the first failure. Finally, we use numerical examples to verify the validity of our theoretical results and indicate how some key system parameters

influence the performance measures of the PBFT-based blockchain system with repairable voting nodes.

We further develop the research lines that apply the Markov process and queueing theory to provide the performance analysis of blockchain systems under different consensus [18, 19, 23, 25], where the computation is supported by the RG-factorization technique [64]. Based on this, we are optimistic to believe that the methodology and results given in this paper can be applied to dealing with more general PBFT-based blockchain systems in practice, and develop some effective algorithms to enhance the throughput, security, and reliability of the PBFT-based blockchain systems from the purpose of many actual uses.

Along these research lines, we will continue our future research in the following directions:

—When the lifetime or/and repair time of a voting node is of phase type, an interesting future research is to focus on finding efficient algorithms to deal with the multi-dimensional Markov processes with a block structure corresponding to the PBFT-based blockchain systems.

—Setting up reward functions with respect to cost structure, transaction fee, block reward, blockchain security, and so forth. It is very interesting in our future study to develop stochastic optimization, Markov decision processes, and stochastic game models in the study of PBFT-based blockchain systems.

—In the direction of stochastic optimization, dynamic control, and Markov decision processes for the PBFT-based blockchain systems, develop efficient algorithms for dealing with the optimal policy from the throughput, security, and reliability.

Acknowledgment

This work was supported by the National Natural Science Foundation of China under grant No. 71932002.

References

- [1] M. Pease, R. Shostak, and L. Lamport, “Reaching agreement in the presence of faults,” *Journal of the ACM (JACM)*, vol. 27, no. 2, pp. 228-234, 1980.

- [2] L. Lamport, R. Shostak, and M. Pease, “The Byzantine generals problem,” *ACM Transactions on Programming Languages and Systems*, vol. 4, no. 3, pp. 382-401, 1982.
- [3] L. Lamport, “The weak Byzantine generals problem,” *Journal of the ACM*, vol. 30, no. 3, pp. 668-676, 1983.
- [4] S. Nakamoto, “Bitcoin: A peer-to-peer electronic cash system,” pp. 1-9, 2008. [Online]. Available: <http://bitcoin.org/bitcoin.pdf>.
- [5] V. Buterin, “Ethereum whitepaper,” 2013. [Online]. Available: <https://github.com/ethereum/wiki/wiki/White-Paper>.
- [6] S. Bano, A. Sonnino, M. Al-Bassam, S. Azouvi, P. McCorry, S. Meiklejohn, and G. Danezis, “Consensus in the age of blockchains,” arXiv preprint, 2017, arXiv:1711.03936.
- [7] C. Cachin and M. Vukolić, “Blockchain consensus protocols in the wild,” arXiv preprint, 2017, arXiv:1707.01873.
- [8] M. Correia, G. S. Veronese, N. F. Neves, and P. Verissimo, “Byzantine consensus in asynchronous message-passing systems: a survey,” *International Journal of Critical Computer-Based Systems*, vol. 2, no. 2, pp. 141-161, 2011.
- [9] M. Vukolić, “The quest for scalable blockchain fabric: Proof-of-work vs. BFT replication,” in *Open Problems in Network Security: IFIP WG 11.4 International Workshop, iNetSec 2015*, Zurich, Switzerland, October 29, 2015, Springer International Publishing, 2016, pp. 112-125.
- [10] V. Gramoli, “From blockchain consensus back to Byzantine consensus,” *Future Generation Computer Systems*, vol. 107, pp. 760-769, 2020.
- [11] C. Berger and H. P. Reiser, “Scaling byzantine consensus: A broad analysis,” in *Proceedings of the 2nd workshop on scalable and resilient infrastructures for distributed ledgers*, 2018, pp. 13-18.
- [12] S. Gupta, J. Hellings, S. Rahnama, and M. Sadoghi, “An in-depth look of BFT consensus in blockchain: Challenges and opportunities,” in *Proceedings of the 20th international middleware conference tutorials*, 2019, pp. 6-10.

- [13] N. Stifter, A. Judmayer, and E. Weippl, “Revisiting practical byzantine fault tolerance through blockchain technologies,” *Security and Quality in Cyber-Physical Systems Engineering: With Forewords by Robert M. Lee and Tom Gilb*, pp. 471-495, 2019.
- [14] S. Alqahtani and M. Demirbas, “Bottlenecks in blockchain consensus protocols,” *2021 IEEE International Conference on Omni-Layer Intelligent Systems (COINS)*, IEEE, 2021, pp. 1-8.
- [15] X. Zheng and W. Feng, “Research on practical byzantine fault tolerant consensus algorithm based on blockchain,” *Journal of Physics: Conference Series*, vol. 1802, no. 3, pp. 032022, 2021.
- [16] B. Gan, Q. Wu, X. Li, and Y. Zhou, “Classification of Blockchain Consensus Mechanisms Based on PBFT Algorithm,” in *2021 International Conference on Computer Engineering and Application (ICCEA)*, IEEE, 2021, pp. 26-29.
- [17] I. Eyal, and E. G. Sirer, “Majority is not enough: Bitcoin mining is vulnerable,” *Communications of the ACM*, vol. 61, no. 7, pp. 95-102, 2018.
- [18] Q. L. Li, J. Y. Ma, and Y. X. Chang, “Blockchain queue theory,” in *International Conference on Computational Social Networks*, Springer, Lecture Notes in Computer Science book series, 2018, vol. 11280, pp. 25-40.
- [19] Q. L. Li, J. Y. Ma, Y. X. Chang, F. Q. Ma, and H. B. Yu, “Markov processes in blockchain systems,” *Computational Social Networks*, vol. 6, no. 1, pp. 1-28, 2019.
- [20] J. Göbel, H. P. Keeler, A. E. Krzesinski, and P. G. Taylor, “Bitcoin blockchain dynamics: The selfish-mine strategy in the presence of propagation delay,” *Performance Evaluation*, vol. 104, pp. 23-41, 2016.
- [21] K. Javier, and B. Fralix, “A further study of some Markovian Bitcoin models from Göbel et al.,” *Stochastic Models*, vol. 36, no. 2, pp. 223-250, 2020.
- [22] Q. L. Li, Y. X. Chang, X. Wu, and G. Zhang, “A new theoretical framework of pyramid markov processes for blockchain selfish mining,” *Journal of Systems Science and Systems Engineering*, vol. 30, no. 6, pp. 667-711, 2021.

- [23] X. S. Song, Q. L. Li, Y. X. Chang, and C. Zhang, "A Markov process theory for network growth processes of DAG-based blockchain systems," arXiv preprint, 2022, arXiv:2209.01458.
- [24] F. Q. Ma, Q. L. Li, Y. H. Liu, and Y. X. Chang, "Stochastic performance modeling for practical byzantine fault tolerance consensus in the blockchain," *Peer-to-Peer Networking and Applications*, vol. 15, no. 6, pp. 2516-2528, 2022.
- [25] Y. X. Chang, Q. L. Li, Q. Wang, and X. S. Song, "Dynamic Practical Byzantine Fault Tolerance and Its Blockchain System: A Large-Scale Markov Modeling," arXiv preprint, 2022, arXiv:2210.14003.
- [26] M. Nischwitz, M. Esche, and F. Tschorsch, "Bernoulli meets PBFT: Modeling BFT protocols in the presence of dynamic failures," in *2021 16th Conference on Computer Science and Intelligence Systems*, IEEE, 2021, pp. 291-300.
- [27] X. Hao, L. Yu, Z. Liu, L. Zhen, and G. Dawu, "Dynamic practical byzantine fault tolerance," in *The 2018 IEEE Conference on Communications and Network Security*, 2018, pp. 1-8.
- [28] R. D. Schlichting and F. B. Schneider, "Fail-stop processors: An approach to designing fault-tolerant computing systems," *ACM Transactions on Computer Systems*, vol. 1, no. 3, pp. 222-238, 1983.
- [29] R. Reischuk, "A new solution for the Byzantine generals problem," *Information and Control*, vol. 64, no. 1-3, pp. 23-42, 1985.
- [30] J. P. Martin and L. Alvisi, "Fast Byzantine consensus," *IEEE Transactions on Dependable and Secure Computing*, vol. 3, no. 3, pp. 202-215, 2006.
- [31] G. S. Veronese, M. Correia, A. N. Bessani, L. C. Lung, and P. Verissimo, "Efficient byzantine fault-tolerance," *IEEE Transactions on Computers*, vol. 62, no. 1, pp. 16-30, 2011.
- [32] D. Malkhi, K. Nayak, and L. Ren, "Flexible byzantine fault tolerance," *Proceedings of the 2019 ACM SIGSAC conference on computer and communications security*, 2019, pp. 1041-1053.

- [33] M. Castro and B. Liskov, "Practical Byzantine fault tolerance," in *Proceedings of the Third Symposium on Operating Systems Design and Implementation*, 1999, pp: 173-186.
- [34] M. Castro and B. Liskov, "Practical Byzantine fault tolerance and proactive recovery," *ACM Transactions on Computer Systems*, vol. 20, no. 4, pp. 398-461, 2002.
- [35] G. Yu, B. Wu, and X. Niu, "Improved blockchain consensus mechanism based on PBFT algorithm," in *2020 2nd International Conference on Advances in Computer Technology, Information Science and Communications (CTISC)*, IEEE, 2020, pp. 14-21.
- [36] Q. T. Thai, J. C. Yim, T. W. Yoo, H. K. Yoo, J. Y. Kwak, and S. M. Kim, "Hierarchical Byzantine fault-tolerance protocol for permissioned blockchain systems," *The Journal of Supercomputing*, vol. 75, no. 11, pp. 7337-7365, 2019.
- [37] T. Crain, V. Gramoli, M. Larrea, and M. Raynal, "Dbft: Efficient leaderless byzantine consensus and its application to blockchains," in *2018 IEEE 17th International Symposium on Network Computing and Applications (NCA)*, IEEE, 2018, pp. 1-8.
- [38] J. Chen, X. Zhang, and P. Shangguan, "Improved PBFT algorithm based on reputation and voting mechanism," in *Journal of Physics: Conference Series*, IOP Publishing, 2020, vol. 1486, no. 3, pp. 032023.
- [39] P. Li, G. Wang, X. Chen, F. Long, and W. Xu, "Gosig: a scalable and high-performance byzantine consensus for consortium blockchains," in *Proceedings of the 11th ACM Symposium on Cloud Computing*, 2020, pp. 223-237.
- [40] Y. Li, Z. Wang, J. Fan, Y. Zheng, Y. Luo, C. Deng, and J. Ding, "An extensible consensus algorithm based on PBFT," in *2019 International conference on cyber-enabled distributed computing and knowledge discovery (CyberC)*, IEEE, 2019, pp. 17-23.
- [41] H. Wang, K. Guo, and Q. Pan, "Byzantine fault tolerance consensus algorithm based on voting mechanism," *Journal of Computer Applications*, vol. 39, no. 6, pp. 1766, 2019.

- [42] Y. Wang, Z. Song, and T. Cheng, "Improvement research of PBFT consensus algorithm based on credit," in *Blockchain and Trustworthy Systems: First International Conference, BlockSys 2019*, Guangzhou, China, 2019, pp. 47-59.
- [43] W. Tong, X. Dong, and J. Zheng, "Trust-pbft: A peertrust-based practical byzantine consensus algorithm," in *2019 International Conference on Networking and Network Applications (NaNA)*, IEEE, 2019, pp. 344-349.
- [44] S. Gao, T. Yu, J. Zhu, and W. Cai, "T-PBFT: An EigenTrust-based practical Byzantine fault tolerance consensus algorithm," *China Communications*, vol. 16, no. 12, pp. 111-123, 2019.
- [45] S. Sakho, J. Zhang, F. Essaf, K. Badiss, T. Abide, and J. K. Kiprop, "Research on an improved practical byzantine fault tolerance algorithm," in *2020 2nd International Conference on Advances in Computer Technology, Information Science and Communications (CTISC)*, IEEE, 2020, pp. 176-181.
- [46] G. Christofi, "Study of consensus protocols and improvement of the Delegated Byzantine Fault Tolerance (DBFT) algorithm," Master's thesis, Universitat Politècnica de Catalunya, 2019.
- [47] G. G. Gueta, I. Abraham, S. Grossman, et al., "Sbft: a scalable and decentralized trust infrastructure," in *2019 49th Annual IEEE/IFIP international conference on dependable systems and networks (DSN)*, IEEE, 2019, pp. 568-580.
- [48] L. Lao, X. Dai, B. Xiao, et al., "G-PBFT: a location-based and scalable consensus protocol for IOT-Blockchain applications," in *2020 IEEE international parallel and distributed processing symposium (IPDPS)*, IEEE, 2020, pp. 664-673.
- [49] Y. Meshcheryakov, A. Melman, O. Evsutin, V. Morozov, and Y. Koucheryavy, "On performance of PBFT for IoT-applications with constrained devices," arXiv preprint, 2021, arXiv:2104.05026.
- [50] X. Yuan, F. Luo, M. Z. Haider, Z. Chen, and Y. Li, "Efficient Byzantine consensus mechanism based on reputation in IoT blockchain," *Wireless Communications and Mobile Computing*, pp. 1-14, 2021.

- [51] W. Hu, Y. Hu, W. Yao, and H. Li, “A blockchain-based Byzantine consensus algorithm for information authentication of the Internet of vehicles,” *IEEE Access*, vol. 7, pp. 139703-139711, 2019.
- [52] J. Lim, T. Suh, J. Gil, and H. Yu, “Scalable and leaderless Byzantine consensus in cloud computing environments,” *Information Systems Frontiers*, vol. 16, no. 1, pp. 19-34, 2014.
- [53] A. Sheikh, V. Kamuni, A. Urooj, S. Wagh, N. Singh, and D. Patel, “Secured energy trading using byzantine-based blockchain consensus,” *IEEE Access*, vol. 8, pp. 8554-8571, 2019.
- [54] C. Fan, S. Ghaemi, H. Khazaei, and P. Musilek, “Performance evaluation of blockchain systems: A systematic survey,” *IEEE Access*, vol. 8, pp. 126927-126950, 2020.
- [55] M. Dabbagh, K. K. R. Choo, A. Beheshti, M. Tahir, and N. S. Safa, “A survey of empirical performance evaluation of permissioned blockchain platforms: Challenges and opportunities,” *computers and security*, vol. 100, pp. 102078, 2021.
- [56] Y. Hao, Y. Li, X. Dong, L. Fang, and P. Chen, “Performance analysis of consensus algorithm in private blockchain,” in *2018 IEEE Intelligent Vehicles Symposium (IV)*, IEEE, pp. 280-285, 2018.
- [57] H. Sukhwani, J. M. Martínez, X. Chang, K. S. Trivedi, and A. Rindos, “Performance modeling of PBFT consensus process for permissioned blockchain network (hyperledger fabric),” in *2017 IEEE 36th symposium on reliable distributed systems (SRDS)*, IEEE, pp. 253-255, 2017.
- [58] T. Lorünser, B. Rainer, and F. Wohner, “Towards a Performance Model for Byzantine Fault Tolerant Services,” *CLOSER*, pp. 178-189, 2022.
- [59] S. Pongnumkul, C. Siripanpornchana, and S. Thajchayapong, “Performance analysis of private blockchain platforms in varying workloads,” in *2017 26th International Conference on Computer Communication and Networks (ICCCN)*, IEEE, 2017, pp. 1-6.

- [60] A. A. Monrat, O. Schelén, and K. Andersson, “Performance evaluation of permissioned blockchain platforms,” in *2020 IEEE Asia-Pacific Conference on Computer Science and Data Engineering (CSDE)*, IEEE, 2020, pp. 1-8.
- [61] A. Ahmad, M. Saad, J. Kim, D. Nyang, and D. Mohaisen, “Performance evaluation of consensus protocols in blockchain-based audit systems,” in *2021 International Conference on Information Networking (ICOIN)*, IEEE, pp. 654-656, 2021.
- [62] K. Zheng, Y. Liu, C. Dai, Y. Duan, and X. Huang, “Model checking PBFT consensus mechanism in healthcare blockchain network,” in *2018 9th International conference on information technology in medicine and education (ITME)*, IEEE, pp. 877-881, 2018.
- [63] M. F. Neuts, “Matrix-Geometric Solutions in Stochastic Models: An Algorithmic Approach,” The Johns Hopkins University Press, 1981.
- [64] Q. L. Li, “Constructive Computation in Stochastic Models with Applications: The RG-Factorizations,” Springer, 2010.

Two Appendixes

We provide two appendixes for the two infinitesimal generators Θ given in Subsection 4.2 and Q given in Subsection 6.2. Our purpose is to increase the readability of the main paper.

Appendix A: The infinitesimal generator Θ

$$\Theta = \begin{pmatrix} 0 & 0 \\ S^0 & S \end{pmatrix}, S^0 + S\mathbf{e} = 0,$$

where,

$$S^0 = \begin{pmatrix} S_0^0 \\ S_1^0 \\ \vdots \\ S_{2n-1}^0 \\ S_{2n}^0 \end{pmatrix}, S_k^0 = \begin{pmatrix} S_{k,0}^0 \\ S_{k,1}^0 \\ \vdots \\ S_{k,n-1}^0 \\ S_{k,n}^0 \end{pmatrix}, 0 \leq k \leq 2n;$$

$$S_{k,i}^0 = \begin{pmatrix} 0 \\ \vdots \\ 0 \\ (N-k-n)(\theta + \gamma q) \end{pmatrix}_{(n+1-i) \times 1}, \quad 0 \leq i \leq n-1,$$

$$S_{k,n}^0 = (N-k-n)(\theta + \gamma q);$$

$$S = \begin{pmatrix} S_{0,0}^{(k)} & S_{0,1}^{(k)} & & & & \\ & S_{1,1}^{(k)} & S_{1,2}^{(k)} & & & \\ & & S_{2,2}^{(k)} & S_{2,3}^{(k)} & & \\ & & & \ddots & \ddots & \\ & & & & S_{2n-1,2n-1}^{(k)} & S_{2n-1,2n}^{(k)} \\ & & & & & S_{2n,2n}^{(k)} \end{pmatrix},$$

for $0 \leq k \leq 2n-1$,

$$S_{k,k+1} = \begin{pmatrix} F_{0,0}^{(k)} & & & \\ & F_{1,1}^{(k)} & & \\ & & \ddots & \\ & & & F_{n,n}^{(k)} \end{pmatrix},$$

for $0 \leq i \leq n$,

$$F_{i,i}^{(k)} = \begin{pmatrix} (N-k-i)\gamma p & & & \\ & (N-k-i-1)\gamma p & & \\ & & \ddots & \\ & & & (N-k-n)\gamma p \end{pmatrix}_{(n+1-i) \times (n+1-i)};$$

for $0 \leq k \leq 2n-1$,

$$S_{k,k} = \begin{pmatrix} G_{0,0}^{(k)} & G_{0,1}^{(k)} & & & \\ & G_{1,1}^{(k)} & G_{1,2}^{(k)} & & \\ & & \ddots & \ddots & \\ & & & G_{n-1,n-1}^{(k)} & G_{n-1,n}^{(k)} \\ & & & & G_{n,n}^{(k)} \end{pmatrix},$$

for $0 \leq i \leq n-1$,

$$G_{i,i+1}^{(k)} = \begin{pmatrix} (N-k-i)\gamma q & & & & \\ & (N-k-i-1)\gamma q & & & \\ & & \ddots & & \\ & & & (N-k-n+1)\gamma q & \\ & & & & 0 \end{pmatrix}_{(n+1-i) \times (n-i)},$$

$$G_{i,i}^{(k)} = \begin{pmatrix} c_{k,i,0} & (N-k-i)\theta & & & \\ \mu & c_{k,i,1} & (N-k-i-1)\theta & & \\ & \ddots & \ddots & \ddots & \\ & & (n-i-1)\mu & c_{k,i,n-i-1} & (N-k-n+1)\theta \\ & & & (n-i)\mu & c_{k,i,n-i} \end{pmatrix}_{(n+1-i) \times (n+1-i)},$$

$$c_{k,i,m} = -[(N-k-i-m)(\theta + \gamma) + m\mu], 0 \leq m \leq n-i;$$

$$G_{n,n}^{(k)} = -(N-k-n)(\theta + \gamma);$$

$$S_{2n,2n} = \begin{pmatrix} H_{0,0} & H_{0,1} & & & \\ & H_{1,1} & H_{1,2} & & \\ & & \ddots & \ddots & \\ & & & H_{n-1,n-1} & H_{n-1,n} \\ & & & & H_{n,n} \end{pmatrix},$$

for $0 \leq i \leq n-1$,

$$H_{i,i+1} = \begin{pmatrix} (n+1-i)\gamma q & & & & \\ & (n-i)\gamma q & & & \\ & & \ddots & & \\ & & & 2\gamma q & \\ & & & & 0 \end{pmatrix}_{(n+1-i) \times (n-i)},$$

$$H_{i,i} = \begin{pmatrix} f_{i,0} & (n+1-i)\theta & & & \\ \mu & f_{i,1} & (n-i)\theta & & \\ & \ddots & \ddots & \ddots & \\ & & (n-i-1)\mu & f_{i,n-i-1} & 2\theta \\ & & & (n-i)\mu & f_{i,n-i} \end{pmatrix}_{(n+1-i) \times (n+1-i)},$$

$$f_{i,m} = -[(n+1-i-m)(\theta + \gamma q) + m\mu], 0 \leq m \leq n-i-1,$$

$$f_{i,n-i} = -[(N-k-n)\gamma p + (n-i)\mu];$$

$$H_{n,n} = -(\theta + \gamma q).$$

Appendix B: The infinitesimal generator Q

$$Q = \begin{pmatrix} Q_{0,0} & Q_{0,1} & & & & & \\ Q_{1,0} & Q_{1,1} & Q_{1,2} & & & & \\ Q_{2,0} & & Q_{2,2} & Q_{2,3} & & & \\ \vdots & & & \ddots & \ddots & & \\ Q_{2n,0} & & & & Q_{2n,2n} & Q_{2n,2n+1} & \\ Q_{2n+1,0} & & & & & & Q_{2n+1,2n+1} \end{pmatrix},$$

where,

$$Q_{2n+1,0} = \begin{pmatrix} J_{0,0} \\ J_{1,0} \\ \vdots \\ J_{n,0} \end{pmatrix}_{\left(\sum_{i=1}^{n+1} i\right) \times \left(\sum_{i=1}^{n+2} i\right)},$$

$$J_{i,0} = \begin{pmatrix} \beta \\ \beta \\ \vdots \\ \beta \end{pmatrix}_{(n+1-i) \times (n+2)}, \quad 0 \leq i \leq n;$$

$$Q_{2n+1,2n+1} = \begin{pmatrix} K_{0,0} & K_{0,1} & & & & & \\ & K_{1,1} & K_{1,2} & & & & \\ & & & \ddots & \ddots & & \\ & & & & K_{n-1,n-1} & K_{n-1,n} & \\ & & & & & & K_{n,n} \end{pmatrix},$$

for $0 \leq i \leq n-1$,

$$K_{i,i+1} = \begin{pmatrix} (n-i)\gamma q & & & & & & \\ & (n-i-1)\gamma q & & & & & \\ & & \ddots & & & & \\ & & & & \gamma q & & \\ & & & & & & 0 \end{pmatrix}_{(n+1-i) \times (n-i)},$$

$$K_{i,i} = \begin{pmatrix} a_{i,0} & (n-i)\theta & & & \\ \mu & a_{i,1} & (n-i-1)\theta & & \\ & \ddots & \ddots & \ddots & \\ & & (n-i-1)\mu & a_{i,n-i-1} & \theta \\ & & & (n-i)\mu & a_{i,n-i} \end{pmatrix}_{(n+1-i) \times (n+1-i)} ;$$

$$a_{i,m} = -[(n-i-m)(\theta + \gamma q) + m\mu + \beta], \quad 0 \leq m \leq n-i,$$

$$K_{n,n} = -\beta;$$

for $1 \leq k \leq 2n$,

$$Q_{k,0} = \begin{pmatrix} A_{0,0} \\ A_{1,0} \\ \vdots \\ A_{n+1,0} \end{pmatrix}_{\left(\sum_{i=1}^{n+2} i\right) \times \left(\sum_{i=1}^{n+2} i\right)},$$

$$A_{i,0} = \begin{pmatrix} 0 \\ \vdots \\ 0 \\ \beta \end{pmatrix}_{(n+2-i) \times (n+2)}, \quad 0 \leq i \leq n,$$

$$A_{n+1,0} = (\beta, 0, 0, \dots, 0)_{1 \times (n+2)};$$

for $0 \leq k \leq 2n-1$,

$$Q_{k,k+1} = \begin{pmatrix} B_{0,0}^{(k)} & & & & \\ & B_{1,1}^{(k)} & & & \\ & & \ddots & & \\ & & & B_{n,n}^{(k)} & \\ & & & & 0 \end{pmatrix},$$

for $0 \leq i \leq n$,

$$B_{i,i}^{(k)} = \begin{pmatrix} (N-k-i)\gamma p & & & & \\ & (N-k-i-1)\gamma p & & & \\ & & \ddots & & \\ & & & (N-k-n)\gamma p & \\ & & & & 0 \end{pmatrix}_{(n+2-i) \times (n+2-i)} ;$$

$$Q_{2n,2n+1} = \begin{pmatrix} C_{0,0} & & & \\ & C_{1,1} & & \\ & & \ddots & \\ & & & C_{n,n} \\ & & & & 0 \end{pmatrix},$$

where,

$$C_{i,i} = \begin{pmatrix} (n+1-i)\gamma p & & & \\ & (n-i)\gamma p & & \\ & & \ddots & \\ & & & \gamma p \\ & & & & 0 \end{pmatrix}_{(n+2-i) \times (n+1-i)}, \quad 0 \leq i \leq n;$$

$$Q_{0,0} = \begin{pmatrix} D_{0,0} & D_{0,1} & & & & \\ D_{1,0} & D_{1,1} & D_{1,2} & & & \\ D_{2,0} & & D_{2,2} & D_{2,3} & & \\ \vdots & & & \ddots & \ddots & \\ D_{n,0} & & & & D_{n,n} & D_{n,n+1} \\ D_{n+1,0} & & & & & D_{n+1,n+1} \end{pmatrix},$$

$$D_{n+1,0} = (\beta, 0, \dots, 0)_{1 \times (n+2)}, D_{n+1,n+1} = -\beta,$$

$$D_{i,0} = \begin{pmatrix} 0 \\ \vdots \\ 0 \\ \beta \end{pmatrix}_{(n+2-i) \times (n+2)}, \quad 1 \leq i \leq n,$$

for $0 \leq i \leq n$,

$$D_{i,i+1} = \begin{pmatrix} (N-i)\gamma q & & & & \\ & (N-i-1)\gamma q & & & \\ & & \ddots & & \\ & & & (N-n)\gamma q & \\ & & & & 0 \end{pmatrix}_{(n+2-i) \times (n+1-i)};$$

$$b_{i,m} = -[(N-i-m)(\theta + \gamma) + m\mu], \quad 0 \leq m \leq n-i,$$

$$d_i = (n+1-i)\mu, \quad 0 \leq i \leq n,$$

$$D_{0,0} = \begin{pmatrix} -b_{0,0} & N\theta & & & & \\ \mu & -b_{0,1} & (N-1)\theta & & & \\ & \ddots & \ddots & \ddots & & \\ & & n\mu & -b_{0,n} & (N-n)\theta & \\ \beta & & & (n+1)\mu & -d_0 - \beta & \end{pmatrix}_{(n+2) \times (n+2)},$$

for $1 \leq i \leq n$,

$$D_{i,i} = \begin{pmatrix} -b_{i,0} & (N-i)\theta & & & & \\ \mu & -b_{i,1} & (N-i-1)\theta & & & \\ & \ddots & \ddots & \ddots & & \\ & & (n-i)\mu & -b_{i,n-i} & (N-n)\theta & \\ & & & d_i & -d_i - \beta & \end{pmatrix}_{(n+2-i) \times (n+2-i)};$$

for $1 \leq k \leq 2n$,

$$Q_{k,k} = \begin{pmatrix} E_{0,0}^{(k)} & E_{0,1}^{(k)} & & & & \\ & E_{1,1}^{(k)} & E_{1,2}^{(k)} & & & \\ & & E_{2,2}^{(k)} & E_{2,3}^{(k)} & & \\ & & & \ddots & \ddots & \\ & & & & E_{n,n}^{(k)} & E_{n,n+1}^{(k)} \\ & & & & & E_{n+1,n+1}^{(k)} \end{pmatrix},$$

$$E_{n+1,n+1}^{(k)} = -\beta,$$

for $0 \leq i \leq n$,

$$E_{i,i+1}^{(k)} = \begin{pmatrix} (N-k-i)\gamma q & & & & & \\ & (N-k-i-1)\gamma q & & & & \\ & & \ddots & & & \\ & & & \ddots & & \\ & & & & (N-k-n)\gamma q & \\ & & & & & 0 \end{pmatrix}_{(n+2-i) \times (n+1-i)},$$

$$E_{i,i}^{(k)} = \begin{pmatrix} -c_{k,i,0} & (N-k-i)\theta & & & \\ \mu & -c_{k,i,1} & (N-k-i-1)\theta & & \\ & \ddots & \ddots & \ddots & \\ & & (n-i)\mu & -c_{k,i,n-i} & (N-k-n)\theta \\ & & & d_i & -d_i - \beta \end{pmatrix}_{(n+2-i) \times (n+2-i)},$$

$c_{k,i,m} = -[(N-k-i-m)(\theta + \gamma) + m\mu], 0 \leq m \leq n-i.$